8.A.5 Nuclear Physics B34 (1971) 41-70. North-Holland Publishing Company

AN IMPROVED PARTIAL WAVE ANALYSIS OF $\bar{K}N \to \bar{K}N$ FROM 800 TO 1200 MeV/c

B. CONFORTO, D. M. HARMSEN *, T. LASINSKI ‡,
R. LEVI-SETTI and M. RAYMUND
The Enrico Fermi Institute and Department of Physics, The University of Chicago, Chicago, Illinois **

E. BURKHARDT, H. FILTHUTH, S. KLEIN,
H. OBERLACK ‡ and H. SCHLEICH
Institut für Hochenergiephysik der Universität Heidelberg ***

Received 2 August 1970
(Revised 7 June 1971)

Abstract: An extensive search for resonant states has been performed through an energy dependent partial wave analysis of $\bar{K}N$ data in the momentum region 777 - 1226 MeV/c. The $K^-p \to K^-p$, $\bar{K}^0n$ differential cross sections, polarization angular distributions and total K^-p cross sections were included in the fit. In addition to the well established hyperons, evidence is reported for a resonant state $\Sigma(1760)$ of $J^P = \frac{1}{2}^-$ and for the assignment $J^P = \frac{3}{2}^+$ for a $\Lambda(1870)$ state previously assigned to $J^P = \frac{1}{2}^+$. From the $K^-p \to K^-p$ differential and total cross sections between 436 and 1226 MeV/c the ratio of the real to the imaginary part of the forward scattering amplitude has been derived as a function of K^- incident momentum. These results are found to be consistent with the predictions of several dispersion relation calculations.

1. INTRODUCTION

Our previous study [1] of the reaction $K^-p \to K^-p$ at twenty three momenta between 777 and 1226 MeV/c, which was based on the analysis of 71 000 two-prong events, has been recently implemented with the analysis of 14 000 additional events. The statistics have been increased by a significant amount at several selected momenta below 1 GeV/c. Such improvement in our data, and the fact that $K^-p \to K^-p$ polarization data [2] in our momentum region have become available, have motivated a new study of hyperon formation in the $\bar{K}N$ channel. Through an energy dependent partial wave analysis of the data, an extensive search for resonant behavior of the

* Now at CERN, Geneva.
‡ Present address: Lawrence Berkeley Laboratory, Berkeley, Ca. 94720.
** Research sponsored by the Air Force Office of Scientific Research Office of Aerospace Research. United States Air Force. Contract No. AF 49 (638) - 1652 and The National Science Foundation.
*** Work supported by the Bundesministerium für Bildung und Wissenschaft.

partial waves has been performed. In addition to the well known resonant states $\frac{3}{2}^-$ $\Lambda(1690)$, $\frac{5}{2}^-$ $\Sigma(1765)$, and $\frac{5}{2}^+$ $\Lambda(1815)$ in our region, we confirm the evidence for a state $\frac{5}{2}^-$ $\Lambda(1830)$ [3-5], propose the existence of a new state $\frac{1}{2}^-$ $\Sigma(1760)$, and indicate a preferred $\frac{3}{2}^+$ assignment to $\Lambda(1870)$, the latter having been previously introduced as a $\frac{7}{2}^+$ state [4]. Finally, the comparison of experimental data for the ratio of the real to the imaginary part of the forward scattering amplitude, with the predictions of several dispersion relation calculations is critically discussed. Preliminary results of this work were reported previously [6].

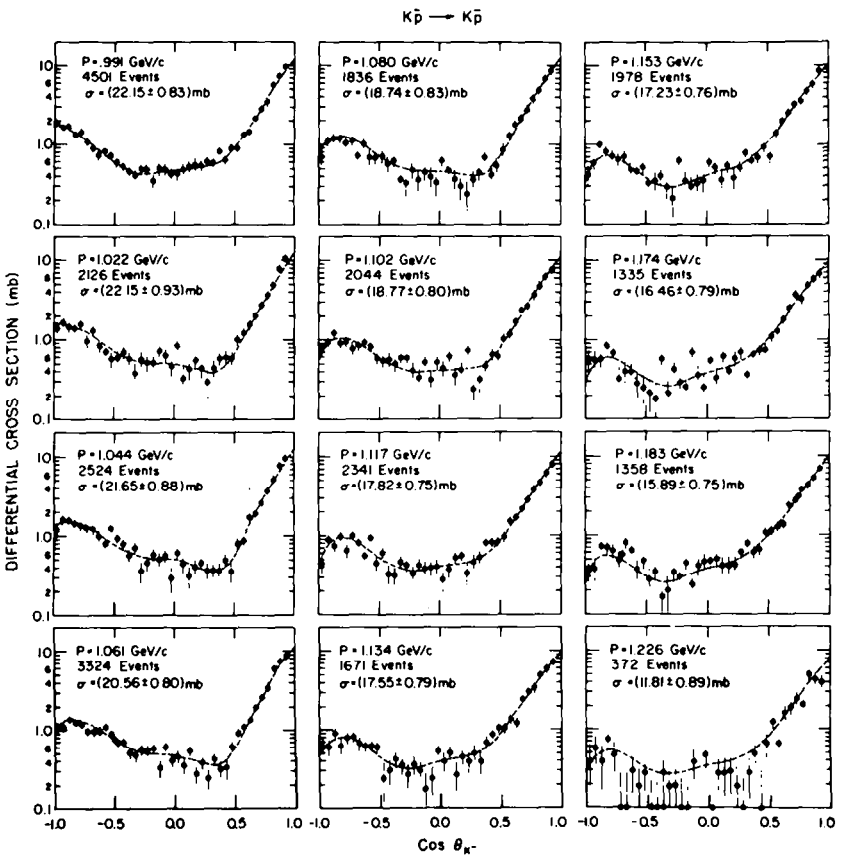

Fig. 1a. Updated elastic differential cross sections from this experiment. The dashed curves represent the best fit to the data in terms of the partial wave analysis discussed in the text.

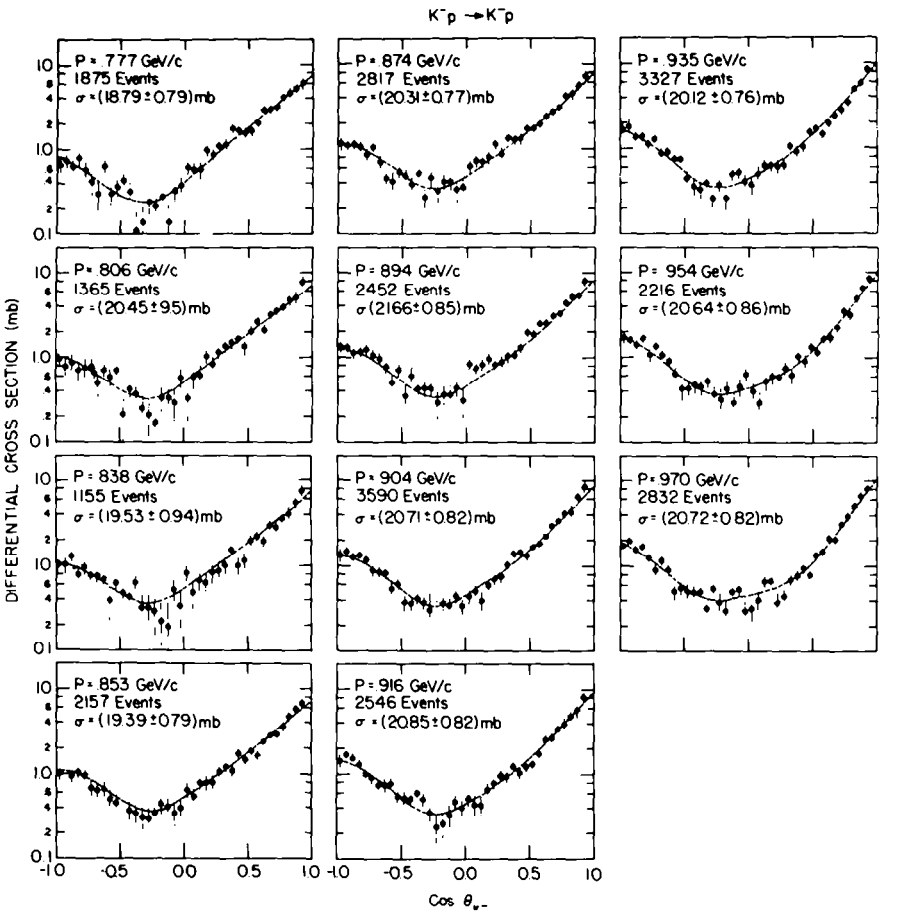

Fig. 1a. (Continued).

2. SEARCH FOR RESONANT STATES

2.1. *New* $K^-p \to K^-p$ *data*

The analysis of two prong events described in ref. [1] has been pursued with the same method to augment the statistics at 15 out of the 23 momenta studied between 777 and 1226 MeV/c. A total of 10 000 $K^-p \to K^-p$ events have been added to our previous statistics of ~42 000 elastic events, mostly at momenta below 1 GeV/c. Our final differential cross sections are given in table 1 and fig. 1a. It should be noticed that the data at 1.022, 1.044, 1.061, 1.080, 1.153, 1.174, 1.183, 1.226 GeV/c are the same as previously given [1]. Although in the partial wave analysis presented here, we will not make use of the Legendre polynomial expansion of the differen-

tial cross sections, the coefficients of such expansions to the 5th and 6th order are given in tables 2a and 2b. They have been derived by the iterative procedure described in ref. [1]. Also contained in these tables are the integrated $K^-p \to K^-p$ cross sections.

2.2. *Partial wave analysis of* $\bar{K}N \to \bar{K}N$

Over the past few years, a part of the $K^-p \to K^-p$ data from our experiment has been used, in conjunction with the corresponding $K^-p \to \bar{K}^0n$ data [7], to analyze the behavior of the $\bar{K}N \to \bar{K}N$ partial wave amplitudes [1, 4, 8, 9]. With the exception of ref. [9], which describes a first step toward an

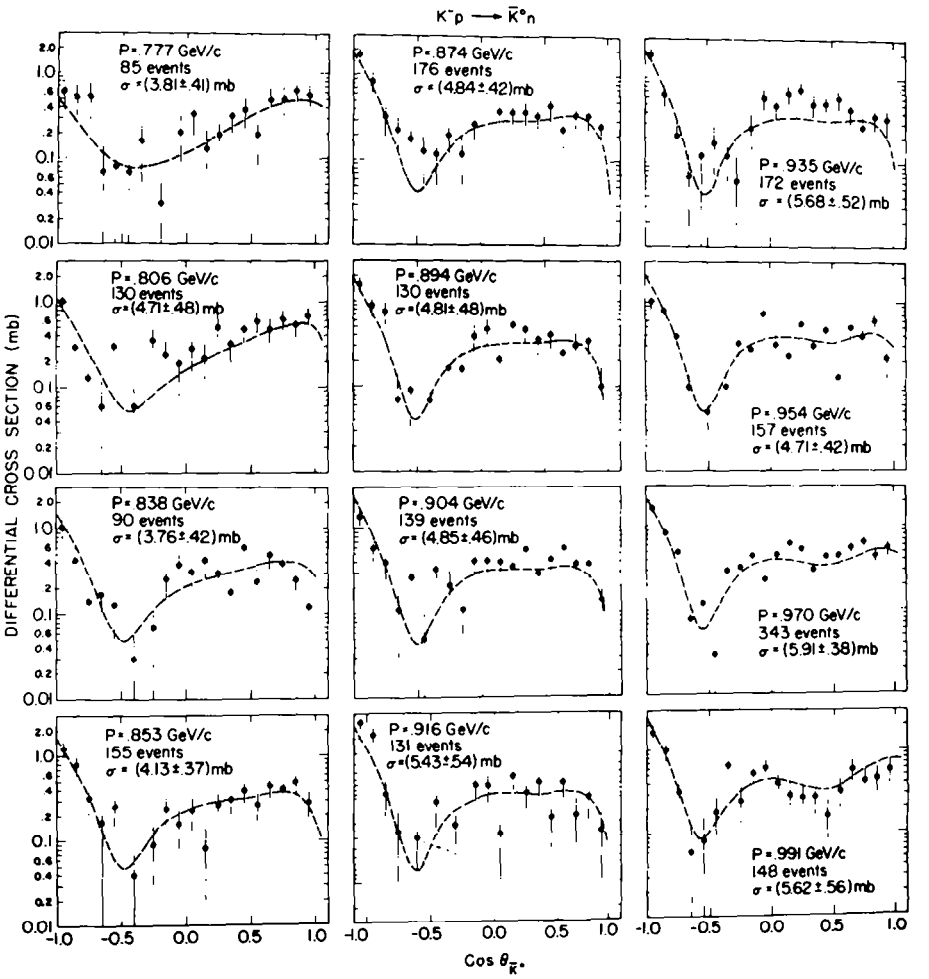

Fig. 1b. Same as fig. 1a for the charge exchange differential cross sections of ref. [7].

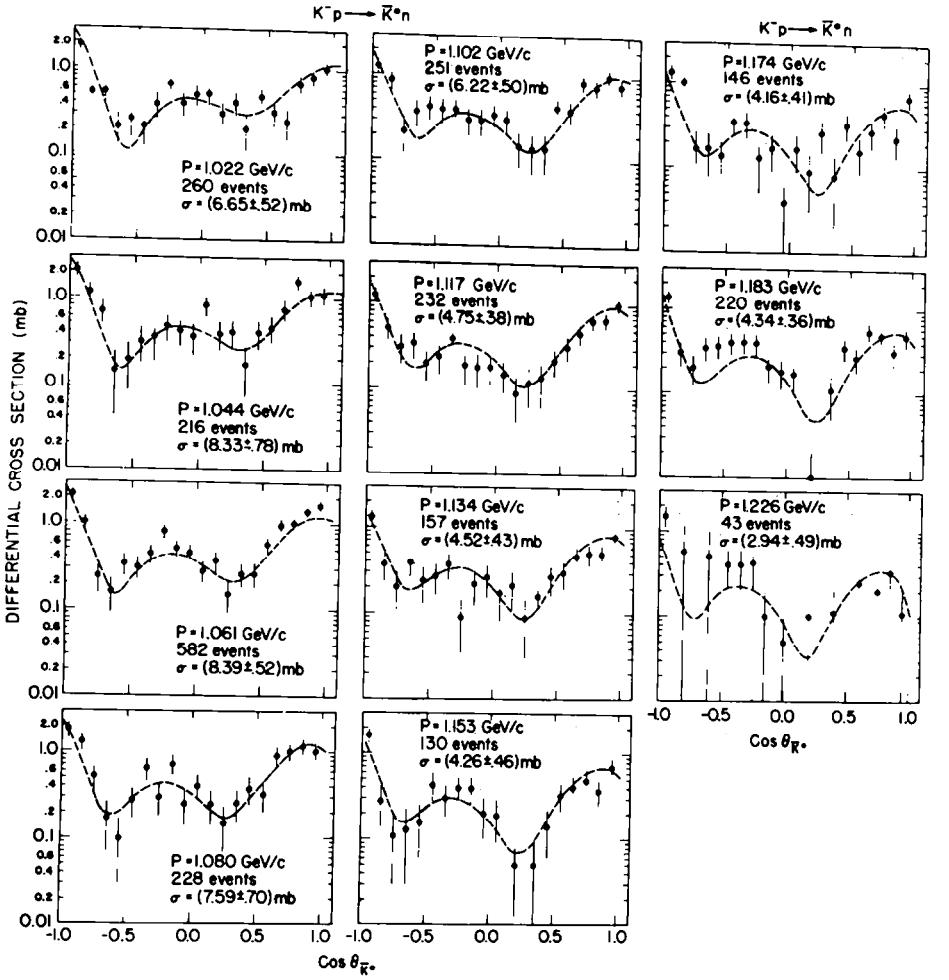

Fig. 1b. (Continued).

energy independent analysis of the data, all other partial wave analyses were based on specific assumptions about the energy dependence of non-resonant and resonant partial waves.

In the present analysis, the energy dependence of the partial waves was parametrized as follows:

a) non-resonant amplitudes: the widely adopted [1, 4, 8] linear expansion in the incident beam momentum was used,

$$T_B = a + b\,(P_K - 1.0\ \text{GeV}/c)\,, \qquad (1)$$

where a and b are complex constants, and P_K is the laboratory beam momentum in GeV/c.

Table 1
Updated differential $K^-p \to K^-p$ cross sections. These supersede those previously reported [1].
$d\sigma/d\Omega$(mb/sr)

$\cos\theta$ (c.m.)	$\Delta(\cos\theta)$	777 MeV/c	806 MeV/c	838 MeV/c	853 MeV/c	874 MeV/c	894 MeV/c
-0.975	0.05	0.667 ± 0.161	0.953 ± 0.195	1.065 ± 0.240	0.957 ± 0.161	1.162 ± 0.195	1.341 ± 0.226
-0.925	0.05	0.749 ± 0.142	0.788 ± 0.191	1.012 ± 0.230	0.544 ± 0.152	1.107 ± 0.159	1.303 ± 0.187
-0.875	0.05	0.638 ± 0.141	0.871 ± 0.198	1.301 ± 0.232	0.906 ± 0.156	1.149 ± 0.157	1.124 ± 0.185
-0.825	0.05	0.805 ± 0.138	0.705 ± 0.197	0.771 ± 0.228	1.010 ± 0.156	1.066 ± 0.153	1.149 ± 0.181
-0.775	0.05	0.589 ± 0.133	0.746 ± 0.191	0.964 ± 0.220	0.958 ± 0.152	0.857 ± 0.146	1.226 ± 0.174
-0.725	0.05	0.416 ± 0.126	0.788 ± 0.182	0.771 ± 0.208	0.673 ± 0.146	1.045 ± 0.137	1.047 ± 0.165
-0.675	0.05	0.305 ± 0.118	0.498 ± 0.170	0.771 ± 0.195	0.621 ± 0.138	0.710 ± 0.128	0.971 ± 0.154
-0.625	0.05	0.645 ± 0.111	0.705 ± 0.157	0.675 ± 0.181	0.647 ± 0.129	0.460 ± 0.118	0.766 ± 0.144
-0.575	0.05	0.305 ± 0.102	0.581 ± 0.143	0.386 ± 0.166	0.492 ± 0.120	0.418 ± 0.108	0.485 ± 0.133
-0.525	0.05	0.365 ± 0.095	0.705 ± 0.129	0.627 ± 0.152	0.440 ± 0.112	0.543 ± 0.099	0.690 ± 0.123
-0.475	0.05	0.454 ± 0.089	0.207 ± 0.117	0.482 ± 0.140	0.725 ± 0.104	0.481 ± 0.092	0.358 ± 0.114
-0.425	0.05	0.337 ± 0.083	0.415 ± 0.107	0.434 ± 0.130	0.362 ± 0.098	0.376 ± 0.086	0.613 ± 0.106
-0.375	0.05	0.111 ± 0.079	0.373 ± 0.100	0.627 ± 0.123	0.337 ± 0.093	0.522 ± 0.082	0.434 ± 0.100
-0.325	0.05	0.140 ± 0.078	0.249 ± 0.097	0.337 ± 0.120	0.311 ± 0.091	0.272 ± 0.081	0.434 ± 0.097
-0.275	0.05	0.253 ± 0.079	0.207 ± 0.098	0.337 ± 0.120	0.285 ± 0.092	0.460 ± 0.082	0.434 ± 0.096
-0.225	0.05	0.222 ± 0.082	0.166 ± 0.104	0.290 ± 0.124	0.362 ± 0.094	0.334 ± 0.085	0.281 ± 0.097
-0.175	0.05	0.278 ± 0.087	0.332 ± 0.112	0.241 ± 0.131	0.440 ± 0.098	0.418 ± 0.090	0.358 ± 0.101
-0.125	0.05	0.140 ± 0.094	0.332 ± 0.122	0.193 ± 0.139	0.414 ± 0.104	0.418 ± 0.096	0.358 ± 0.105
-0.075	0.05	0.333 ± 0.101	0.290 ± 0.134	0.530 ± 0.149	0.337 ± 0.111	0.334 ± 0.103	0.434 ± 0.111
-0.025	0.05	0.365 ± 0.110	0.581 ± 0.146	0.337 ± 0.159	0.388 ± 0.118	0.355 ± 0.110	0.306 ± 0.118
0.025	0.05	0.611 ± 0.119	0.332 ± 0.158	0.819 ± 0.169	0.647 ± 0.125	0.627 ± 0.117	0.843 ± 0.125
0.075	0.05	0.583 ± 0.129	0.581 ± 0.170	0.482 ± 0.178	0.544 ± 0.132	0.731 ± 0.124	0.741 ± 0.133
0.125	0.05	0.583 ± 0.139	0.622 ± 0.182	0.675 ± 0.188	0.777 ± 0.140	0.710 ± 0.130	0.817 ± 0.141
0.175	0.05	0.982 ± 0.151	1.037 ± 0.193	0.627 ± 0.197	0.777 ± 0.147	0.794 ± 0.137	0.945 ± 0.149
0.225	0.05	0.870 ± 0.162	0.829 ± 0.204	0.819 ± 0.206	0.777 ± 0.155	1.149 ± 0.144	0.817 ± 0.157
0.275	0.05	1.083 ± 0.173	1.161 ± 0.216	0.868 ± 0.215	1.036 ± 0.163	0.877 ± 0.151	0.894 ± 0.165
0.325	0.05	1.138 ± 0.186	1.368 ± 0.228	1.012 ± 0.225	1.191 ± 0.171	1.316 ± 0.158	1.022 ± 0.175
0.375	0.05	1.721 ± 0.199	1.493 ± 0.240	1.542 ± 0.235	1.087 ± 0.180	1.254 ± 0.166	1.047 ± 0.185
0.425	0.05	1.665 ± 0.213	1.659 ± 0.254	1.012 ± 0.248	1.709 ± 0.190	1.316 ± 0.175	1.328 ± 0.196
0.475	0.05	1.582 ± 0.228	1.327 ± 0.269	1.157 ± 0.269	1.450 ± 0.202	1.734 ± 0.186	1.992 ± 0.210
0.525	0.05	1.610 ± 0.244	2.032 ± 0.287	1.976 ± 0.281	1.838 ± 0.216	1.734 ± 0.199	1.839 ± 0.225
0.575	0.05	2.021 ± 0.264	2.613 ± 0.308	2.217 ± 0.302	1.631 ± 0.233	1.964 ± 0.214	2.477 ± 0.244
0.625	0.05	2.915 ± 0.282	2.156 ± 0.332	1.976 ± 0.329	2.460 ± 0.253	2.403 ± 0.233	2.503 ± 0.265
0.675	0.05	3.003 ± 0.305	3.193 ± 0.361	3.037 ± 0.361	2.822 ± 0.276	2.695 ± 0.255	3.090 ± 0.291
0.725	0.05	3.115 ± 0.330	3.525 ± 0.394	2.844 ± 0.399	2.848 ± 0.304	3.134 ± 0.281	3.218 ± 0.321
0.775	0.05	4.189 ± 0.555	3.941 ± 0.615	3.477 ± 0.597	3.581 ± 0.515	4.199 ± 0.501	4.400 ± 0.558
0.825	0.05	4.632 ± 0.642	4.767 ± 0.721	4.260 ± 0.707	4.664 ± 0.610	4.524 ± 0.604	5.185 ± 0.664
0.875	0.05	5.388 ± 0.756	5.188 ± 0.877	5.480 ± 0.862	5.864 ± 0.745	5.603 ± 0.739	5.350 ± 0.812
0.925	0.05	5.863 ± 0.972	7.822 ± 1.185	7.480 ± 1.109	6.648 ± 1.010	7.222 ± 1.002	7.968 ± 1.050

Table 1 (continued)

$\cos\theta$ (c.m.)	$\Delta(\cos\theta)$	$d\sigma/d\Omega$(mb/sr) 904 MeV/c	916 MeV/c	935 MeV/c	954 MeV/c	970 MeV/c	991 MeV/c
-0.975	0.05	1.372 ± 0.214	1.429 ± 0.263	1.671 ± 0.234	1.702 ± 0.270	1.732 ± 0.286	1.973 ± 0.258
-0.925	0.05	1.462 ± 0.160	1.677 ± 0.194	1.759 ± 0.175	1.603 ± 0.215	1.972 ± 0.202	1.732 ± 0.170
-0.875	0.05	1.275 ± 0.159	1.606 ± 0.188	1.337 ± 0.172	1.416 ± 0.212	1.591 ± 0.194	1.815 ± 0.166
-0.825	0.05	1.309 ± 0.154	1.276 ± 0.179	1.354 ± 0.166	1.657 ± 0.204	1.697 ± 0.184	1.399 ± 0.159
-0.775	0.05	1.173 ± 0.146	0.992 ± 0.169	1.108 ± 0.157	1.069 ± 0.194	1.251 ± 0.173	1.593 ± 0.149
-0.725	0.05	0.867 ± 0.137	0.803 ± 0.158	1.266 ± 0.147	1.336 ± 0.181	0.891 ± 0.161	1.122 ± 0.138
-0.675	0.05	0.838 ± 0.127	0.732 ± 0.147	0.862 ± 0.135	1.069 ± 0.168	1.167 ± 0.148	0.942 ± 0.127
-0.625	0.05	0.821 ± 0.116	0.732 ± 0.135	0.897 ± 0.123	0.909 ± 0.154	0.912 ± 0.136	0.762 ± 0.115
-0.575	0.05	0.527 ± 0.105	0.756 ± 0.124	0.739 ± 0.111	0.641 ± 0.140	0.509 ± 0.125	0.845 ± 0.104
-0.525	0.05	0.595 ± 0.094	0.543 ± 0.114	0.739 ± 0.099	0.428 ± 0.127	0.547 ± 0.114	0.762 ± 0.094
-0.475	0.05	0.372 ± 0.084	0.520 ± 0.106	0.440 ± 0.089	0.428 ± 0.116	0.505 ± 0.105	0.624 ± 0.086
-0.425	0.05	0.359 ± 0.077	0.496 ± 0.099	0.352 ± 0.080	0.481 ± 0.106	0.488 ± 0.099	0.540 ± 0.080
-0.375	0.05	0.411 ± 0.071	0.591 ± 0.093	0.334 ± 0.075	0.454 ± 0.099	0.509 ± 0.093	0.471 ± 0.076
-0.325	0.05	0.357 ± 0.068	0.496 ± 0.091	0.387 ± 0.071	0.534 ± 0.095	0.318 ± 0.090	0.416 ± 0.075
-0.275	0.05	0.308 ± 0.068	0.354 ± 0.090	0.264 ± 0.071	0.374 ± 0.094	0.551 ± 0.089	0.513 ± 0.075
-0.225	0.05	0.459 ± 0.069	0.236 ± 0.091	0.369 ± 0.074	0.347 ± 0.096	0.379 ± 0.089	0.499 ± 0.078
-0.175	0.05	0.359 ± 0.074	0.260 ± 0.094	0.264 ± 0.078	0.428 ± 0.099	0.297 ± 0.091	0.360 ± 0.081
-0.125	0.05	0.342 ± 0.079	0.331 ± 0.097	0.493 ± 0.084	0.294 ± 0.104	0.505 ± 0.093	0.499 ± 0.085
-0.075	0.05	0.442 ± 0.084	0.472 ± 0.102	0.528 ± 0.090	0.454 ± 0.109	0.530 ± 0.096	0.485 ± 0.088
-0.025	0.05	0.340 ± 0.091	0.402 ± 0.107	0.405 ± 0.095	0.615 ± 0.114	0.297 ± 0.098	0.443 ± 0.092
0.025	0.05	0.442 ± 0.097	0.520 ± 0.112	0.369 ± 0.101	0.401 ± 0.120	0.318 ± 0.101	0.443 ± 0.094
0.075	0.05	0.513 ± 0.103	0.425 ± 0.117	0.510 ± 0.106	0.294 ± 0.124	0.403 ± 0.104	0.485 ± 0.095
0.125	0.05	0.391 ± 0.108	0.425 ± 0.122	0.633 ± 0.111	0.534 ± 0.128	0.657 ± 0.106	0.540 ± 0.096
0.175	0.05	0.595 ± 0.114	0.661 ± 0.128	0.633 ± 0.115	0.588 ± 0.132	0.673 ± 0.108	0.582 ± 0.095
0.225	0.05	0.697 ± 0.120	0.780 ± 0.134	0.598 ± 0.118	0.588 ± 0.135	0.382 ± 0.111	0.554 ± 0.094
0.275	0.05	0.753 ± 0.126	0.945 ± 0.140	0.633 ± 0.122	0.748 ± 0.139	0.445 ± 0.114	0.624 ± 0.092
0.325	0.05	1.020 ± 0.131	0.921 ± 0.147	1.038 ± 0.125	0.615 ± 0.143	0.694 ± 0.118	0.610 ± 0.091
0.375	0.05	1.394 ± 0.138	1.228 ± 0.156	0.897 ± 0.130	1.015 ± 0.148	0.778 ± 0.124	0.831 ± 0.091
0.425	0.05	1.462 ± 0.147	1.039 ± 0.166	1.020 ± 0.136	0.909 ± 0.156	0.954 ± 0.134	0.651 ± 0.094
0.475	0.05	1.309 ± 0.158	1.228 ± 0.179	1.513 ± 0.144	1.336 ± 0.168	0.799 ± 0.145	0.914 ± 0.101
0.525	0.05	1.682 ± 0.171	1.299 ± 0.194	1.689 ± 0.155	1.149 ± 0.183	1.357 ± 0.162	0.914 ± 0.113
0.575	0.05	1.835 ± 0.187	1.748 ± 0.213	1.442 ± 0.170	1.657 ± 0.203	1.472 ± 0.182	1.330 ± 0.131
0.625	0.05	2.260 ± 0.208	2.551 ± 0.235	1.917 ± 0.190	1.684 ± 0.229	2.100 ± 0.208	1.413 ± 0.155
0.675	0.05	2.993 ± 0.233	2.646 ± 0.262	2.357 ± 0.215	2.218 ± 0.260	2.082 ± 0.237	2.134 ± 0.185
0.725	0.05	3.399 ± 0.262	3.378 ± 0.294	2.744 ± 0.245	3.474 ± 0.299	3.113 ± 0.273	2.827 ± 0.224
0.775	0.05	4.062 ± 0.520	3.874 ± 0.512	3.430 ± 0.462	3.127 ± 0.519	3.881 ± 0.512	3.450 ± 0.495
0.825	0.05	4.365 ± 0.640	4.874 ± 0.635	4.925 ± 0.581	4.931 ± 0.646	5.000 ± 0.643	5.803 ± 0.658
0.875	0.05	6.538 ± 0.817	5.330 ± 0.775	5.651 ± 0.750	6.524 ± 0.831	6.727 ± 0.818	7.327 ± 0.884
0.925	0.05	8.471 ± 1.141	8.042 ± 1.082	8.352 ± 1.026	8.423 ± 1.128	8.090 ± 1.099	9.756 ± 1.257

Table 1 (continued)

cos θ (c.m.)	Δ(cos θ)	dσ/dΩ(mb/sr) 1022 MeV/c	1044 MeV/c	1061 MeV/c	1080 MeV/c	1102 MeV/c	1117 MeV/c
-0.975	0.05	1.479 ± 0.280	1.200 ± 0.243	1.099 ± 0.184	0.685 ± 0.172	0.801 ± 0.180	0.444 ± 0.117
-0.925	0.05	1.748 ± 0.228	1.649 ± 0.201	1.123 ± 0.152	1.097 ± 0.175	0.949 ± 0.163	0.884 ± 0.128
-0.875	0.05	1.511 ± 0.225	1.598 ± 0.202	1.406 ± 0.154	1.186 ± 0.185	1.239 ± 0.166	0.729 ± 0.139
-0.825	0.05	1.448 ± 0.218	1.469 ± 0.200	1.280 ± 0.154	1.187 ± 0.188	0.922 ± 0.166	0.972 ± 0.143
-0.775	0.05	1.658 ± 0.208	1.340 ± 0.196	1.192 ± 0.151	1.011 ± 0.186	0.949 ± 0.163	0.635 ± 0.143
-0.725	0.05	0.994 ± 0.196	1.237 ± 0.190	0.979 ± 0.147	1.097 ± 0.180	0.791 ± 0.159	0.994 ± 0.140
-0.675	0.05	1.356 ± 0.184	1.211 ± 0.182	0.958 ± 0.141	0.712 ± 0.172	0.870 ± 0.154	0.810 ± 0.134
-0.625	0.05	0.878 ± 0.172	0.980 ± 0.174	0.976 ± 0.135	1.008 ± 0.162	0.949 ± 0.148	0.547 ± 0.127
-0.575	0.05	0.726 ± 0.161	0.799 ± 0.164	1.090 ± 0.129	0.683 ± 0.153	0.843 ± 0.142	0.928 ± 0.120
-0.525	0.05	0.605 ± 0.151	1.289 ± 0.156	0.888 ± 0.123	0.679 ± 0.143	0.606 ± 0.136	0.438 ± 0.112
-0.475	0.05	0.638 ± 0.143	0.927 ± 0.147	0.712 ± 0.117	0.683 ± 0.135	0.553 ± 0.131	0.597 ± 0.106
-0.425	0.05	0.723 ± 0.136	0.748 ± 0.139	0.713 ± 0.112	0.562 ± 0.127	0.580 ± 0.127	0.328 ± 0.099
-0.375	0.05	0.605 ± 0.132	0.566 ± 0.132	0.516 ± 0.107	0.621 ± 0.121	0.501 ± 0.123	0.306 ± 0.094
-0.325	0.05	0.393 ± 0.130	0.670 ± 0.126	0.481 ± 0.104	0.355 ± 0.117	0.606 ± 0.120	0.460 ± 0.091
-0.275	0.05	0.603 ± 0.130	0.335 ± 0.121	0.574 ± 0.101	0.326 ± 0.114	0.606 ± 0.117	0.416 ± 0.089
-0.225	0.05	0.544 ± 0.131	0.465 ± 0.117	0.569 ± 0.098	0.473 ± 0.112	0.422 ± 0.115	0.328 ± 0.088
-0.175	0.05	0.542 ± 0.132	0.593 ± 0.115	0.588 ± 0.096	0.356 ± 0.111	0.343 ± 0.113	0.420 ± 0.089
-0.125	0.05	0.752 ± 0.133	0.515 ± 0.113	0.337 ± 0.094	0.443 ± 0.111	0.527 ± 0.112	0.376 ± 0.090
-0.075	0.05	0.662 ± 0.134	0.567 ± 0.111	0.623 ± 0.093	0.386 ± 0.111	0.316 ± 0.111	0.376 ± 0.092
-0.025	0.05	0.482 ± 0.135	0.309 ± 0.110	0.411 ± 0.092	0.325 ± 0.111	0.527 ± 0.110	0.398 ± 0.094
0.025	0.05	0.876 ± 0.134	0.618 ± 0.109	0.462 ± 0.090	0.621 ± 0.110	0.448 ± 0.108	0.284 ± 0.096
0.075	0.05	0.334 ± 0.133	0.438 ± 0.107	0.356 ± 0.088	0.473 ± 0.109	0.632 ± 0.107	0.372 ± 0.099
0.125	0.05	0.452 ± 0.130	0.335 ± 0.105	0.554 ± 0.086	0.355 ± 0.108	0.369 ± 0.106	0.530 ± 0.101
0.175	0.05	0.573 ± 0.126	0.386 ± 0.103	0.284 ± 0.083	0.296 ± 0.107	0.422 ± 0.105	0.552 ± 0.103
0.225	0.05	0.453 ± 0.123	0.412 ± 0.100	0.395 ± 0.081	0.236 ± 0.106	0.738 ± 0.105	0.328 ± 0.105
0.275	0.05	0.302 ± 0.120	0.360 ± 0.098	0.248 ± 0.079	0.356 ± 0.106	0.237 ± 0.107	0.464 ± 0.109
0.325	0.05	0.456 ± 0.120	0.335 ± 0.097	0.429 ± 0.079	0.444 ± 0.109	0.316 ± 0.111	0.525 ± 0.113
0.375	0.05	0.603 ± 0.122	0.386 ± 0.099	0.319 ± 0.082	0.680 ± 0.115	0.474 ± 0.118	0.810 ± 0.119
0.425	0.05	0.635 ± 0.130	0.490 ± 0.105	0.338 ± 0.089	0.414 ± 0.126	0.659 ± 0.129	0.817 ± 0.128
0.475	0.05	0.607 ± 0.144	0.387 ± 0.117	0.620 ± 0.100	0.532 ± 0.141	0.632 ± 0.144	0.817 ± 0.140
0.525	0.05	1.026 ± 0.165	0.825 ± 0.136	0.926 ± 0.118	0.830 ± 0.162	1.054 ± 0.164	0.941 ± 0.155
0.575	0.05	1.270 ± 0.194	0.850 ± 0.161	1.085 ± 0.140	1.273 ± 0.189	1.186 ± 0.187	1.488 ± 0.175
0.625	0.05	1.600 ± 0.229	1.649 ± 0.193	1.369 ± 0.168	1.721 ± 0.221	1.687 ± 0.216	1.657 ± 0.200
0.675	0.05	2.083 ± 0.271	1.855 ± 0.233	1.976 ± 0.202	2.046 ± 0.259	2.346 ± 0.250	2.121 ± 0.230
0.725	0.05	2.869 ± 0.320	2.551 ± 0.281	2.614 ± 0.242	2.639 ± 0.303	2.688 ± 0.289	2.779 ± 0.263
0.775	0.05	3.775 ± 0.559	3.711 ± 0.515	3.581 ± 0.486	3.645 ± 0.518	3.637 ± 0.504	3.742 ± 0.476
0.825	0.05	4.997 ± 0.712	5.121 ± 0.677	6.162 ± 0.636	4.629 ± 0.646	4.817 ± 0.625	4.485 ± 0.594
0.875	0.05	7.962 ± 0.923	7.659 ± 0.909	7.408 ± 0.854	6.617 ± 0.834	6.300 ± 0.796	5.934 ± 0.761
0.925	0.05	10.691 ± 1.235	9.565 ± 1.247	8.707 ± 1.157	8.207 ± 1.084	7.393 ± 1.040	7.708 ± 0.996

Table 1 (continued)

$d\sigma/d\Omega$ (mb/sr)

$\cos\theta$ (c.m.)	$\Delta(\cos\theta)$	1134 MeV/c	1153 MeV/c	1174 MeV/c	1183 MeV/c	1226 MeV/c
-0.975	0.05	0.615 ± 0.145	0.403 ± 0.117	0.560 ± 0.115	0.357 ± 0.109	0.408 ± 0.215
-0.925	0.05	0.603 ± 0.148	0.564 ± 0.129	0.574 ± 0.153	0.372 ± 0.135	0.588 ± 0.228
-0.875	0.05	0.905 ± 0.156	0.951 ± 0.139	0.574 ± 0.155	0.716 ± 0.151	0.402 ± 0.233
-0.825	0.05	0.633 ± 0.158	0.770 ± 0.142	0.825 ± 0.151	0.708 ± 0.155	0.767 ± 0.218
-0.775	0.05	0.814 ± 0.156	0.668 ± 0.140	0.682 ± 0.143	0.639 ± 0.154	0.485 ± 0.204
-0.725	0.05	0.814 ± 0.152	0.617 ± 0.134	0.323 ± 0.134	0.475 ± 0.150	0.096 ± 0.184
-0.675	0.05	0.664 ± 0.145	0.668 ± 0.127	0.395 ± 0.123	0.811 ± 0.142	0.102 ± 0.168
-0.625	0.05	0.633 ± 0.138	0.463 ± 0.119	0.395 ± 0.114	0.647 ± 0.134	0.300 ± 0.148
-0.575	0.05	0.633 ± 0.130	0.436 ± 0.111	0.287 ± 0.106	0.370 ± 0.124	0.192 ± 0.130
-0.525	0.05	0.603 ± 0.122	0.489 ± 0.104	0.251 ± 0.100	0.465 ± 0.114	0.287 ± 0.120
-0.475	0.05	0.241 ± 0.115	0.308 ± 0.097	0.215 ± 0.098	0.269 ± 0.107	0.102 ± 0.121
-0.425	0.05	0.302 ± 0.108	0.333 ± 0.093	0.180 ± 0.098	0.341 ± 0.102	0.096 ± 0.121
-0.375	0.05	0.422 ± 0.103	0.387 ± 0.091	0.574 ± 0.101	0.169 ± 0.098	0.287 ± 0.128
-0.325	0.05	0.362 ± 0.100	0.282 ± 0.090	0.214 ± 0.105	0.203 ± 0.097	0.192 ± 0.138
-0.275	0.05	0.271 ± 0.098	0.205 ± 0.091	0.430 ± 0.110	0.341 ± 0.098	0.198 ± 0.149
-0.225	0.05	0.362 ± 0.097	0.591 ± 0.093	0.287 ± 0.116	0.304 ± 0.101	0.096 ± 0.155
-0.175	0.05	0.302 ± 0.097	0.334 ± 0.096	0.251 ± 0.121	0.441 ± 0.104	0.096 ± 0.162
-0.125	0.05	0.181 ± 0.099	0.283 ± 0.099	0.682 ± 0.125	0.235 ± 0.108	0.390 ± 0.167
-0.075	0.05	0.241 ± 0.101	0.308 ± 0.102	0.358 ± 0.128	0.404 ± 0.113	0.0 0.0
-0.025	0.05	0.543 ± 0.103	0.334 ± 0.104	0.251 ± 0.130	0.462 ± 0.116	0.479 ± 0.165
0.025	0.05	0.392 ± 0.106	0.566 ± 0.106	0.538 ± 0.131	0.473 ± 0.122	0.102 ± 0.166
0.075	0.05	0.513 ± 0.108	0.488 ± 0.107	0.323 ± 0.131	0.496 ± 0.124	0.287 ± 0.155
0.125	0.05	0.271 ± 0.111	0.334 ± 0.108	0.609 ± 0.130	0.404 ± 0.128	0.287 ± 0.148
0.175	0.05	0.452 ± 0.114	0.514 ± 0.109	0.395 ± 0.130	0.404 ± 0.131	0.294 ± 0.145
0.225	0.05	0.392 ± 0.118	0.360 ± 0.111	0.574 ± 0.130	0.409 ± 0.135	0.192 ± 0.141
0.275	0.05	0.513 ± 0.123	0.488 ± 0.113	0.682 ± 0.133	0.602 ± 0.138	0.102 ± 0.150
0.325	0.05	0.392 ± 0.130	0.746 ± 0.117	0.359 ± 0.138	0.774 ± 0.143	0.287 ± 0.157
0.375	0.05	0.694 ± 0.138	0.592 ± 0.124	0.645 ± 0.147	0.605 ± 0.150	0.498 ± 0.182
0.425	0.05	0.875 ± 0.150	0.643 ± 0.134	0.716 ± 0.160	0.639 ± 0.161	0.096 ± 0.208
0.475	0.05	1.056 ± 0.165	0.873 ± 0.148	0.717 ± 0.178	1.038 ± 0.174	0.671 ± 0.244
0.525	0.05	1.025 ± 0.184	0.668 ± 0.166	1.076 ± 0.201	1.109 ± 0.192	1.265 ± 0.288
0.575	0.05	1.357 ± 0.208	1.310 ± 0.189	1.255 ± 0.229	1.217 ± 0.214	0.671 ± 0.332
0.625	0.05	1.206 ± 0.236	1.875 ± 0.217	1.756 ± 0.261	1.323 ± 0.242	1.667 ± 0.386
0.675	0.05	2.443 ± 0.269	2.364 ± 0.249	2.404 ± 0.298	2.292 ± 0.273	1.961 ± 0.439
0.725	0.05	3.076 ± 0.307	3.057 ± 0.287	3.478 ± 0.339	2.630 ± 0.310	2.517 ± 0.490
0.775	0.05	3.408 ± 0.515	3.317 ± 0.502	3.119 ± 0.544	3.615 ± 0.503	2.114 ± 0.620
0.825	0.05	4.893 ± 0.629	4.471 ± 0.612	4.662 ± 0.645	4.075 ± 0.603	4.867 ± 0.703
0.875	0.05	5.838 ± 0.791	5.490 ± 0.760	5.619 ± 0.778	5.080 ± 0.730	4.360 ± 0.790
0.925	0.05	7.324 ± 1.013	7.974 ± 1.002	6.492 ± 0.975	6.526 ± 0.941	4.016 ± 0.906

Table 2a

The A_n coefficients in the Legendre expansion $d\sigma/d\Omega = \lambda^2 \Sigma_n A_n P_n(\cos\theta)$. These coefficients were obtained from 5th order least-square fits to the differential cross sections; the probability of each fit is indicated.

	777 MeV/c	806 MeV/c	838 MeV/c	853 MeV/c	874 MeV/c	894 MeV/c
σ_{K^-p} (mb)	18.21 ± 0.71	19.72 ± 0.85	19.11 ± 0.85	18.93 ± 0.70	19.89 ± 0.68	21.59 ± 0.75
A_0	0.693 ± 0.027	0.795 ± 0.034	0.818 ± 0.036	0.834 ± 0.031	0.909 ± 0.031	1.021 ± 0.035
A_1	1.071 ± 0.070	1.164 ± 0.087	1.100 ± 0.092	1.173 ± 0.079	1.216 ± 0.080	1.344 ± 0.092
A_2	1.059 ± 0.094	1.253 ± 0.119	1.352 ± 0.124	1.314 ± 0.107	1.457 ± 0.108	1.704 ± 0.123
A_3	0.390 ± 0.101	0.513 ± 0.128	0.631 ± 0.135	0.649 ± 0.114	0.634 ± 0.116	0.772 ± 0.133
A_4	0.135 ± 0.082	0.181 ± 0.106	0.310 ± 0.114	0.298 ± 0.095	0.378 ± 0.094	0.411 ± 0.107
A_5	0.135 ± 0.061	0.185 ± 0.082	0.205 ± 0.093	0.249 ± 0.073	0.235 ± 0.074	0.281 ± 0.087
$P(\chi^2)$	0.41	0.73	0.75	0.61	0.76	0.61
	904 MeV/c	916 MeV/c	935 MeV/c	954 MeV/c	970 MeV/c	991 MeV/c
σ_{K^-p} (mb)	20.67 ± 0.69	20.21 ± 0.72	19.75 ± 0.65	20.50 ± 0.75	20.71 ± 0.71	20.94 ± 0.67
A_0	0.994 ± 0.033	0.992 ± 0.035	0.999 ± 0.033	1.069 ± 0.039	1.107 ± 0.038	1.156 ± 0.037
A_1	1.321 ± 0.087	1.242 ± 0.092	1.189 ± 0.086	1.321 ± 0.101	1.348 ± 0.100	1.373 ± 0.098
A_2	1.818 ± 0.116	1.810 ± 0.122	1.865 ± 0.114	2.124 ± 0.134	2.298 ± 0.131	2.415 ± 0.127
A_3	0.826 ± 0.124	0.814 ± 0.132	0.872 ± 0.123	1.139 ± 0.145	1.214 ± 0.141	1.462 ± 0.135
A_4	0.486 ± 0.095	0.504 ± 0.104	0.612 ± 0.095	0.793 ± 0.113	0.914 ± 0.107	1.106 ± 0.101
A_5	0.235 ± 0.075	0.208 ± 0.086	0.379 ± 0.079	0.417 ± 0.096	0.371 ± 0.092	0.573 ± 0.084
$P(\chi^2)$	0.74	0.70	0.33	0.62	0.26	0.68

Table 2a (continued)

$d\sigma/d\Omega = \lambda^2 \Sigma_n A_n P_n(\cos\theta)$ for $n = 5$.

	1022 MeV/c	1044 MeV/c	1061 MeV/c	1080 MeV/c	1102 MeV/c	1117 MeV/c
σ_{K^-p} (mb)	22.28 ± 0.84	21.00 ± 0.77	20.28 ± 0.68	18.98 ± 0.74	18.95 ± 0.70	17.82 ± 0.65
A_0	1.287 ± 0.049	1.251 ± 0.046	1.237 ± 0.041	1.188 ± 0.046	1.221 ± 0.045	1.171 ± 0.043
A_1	1.656 ± 0.125	1.540 ± 0.118	1.659 ± 0.108	1.687 ± 0.119	1.720 ± 0.117	1.774 ± 0.110
A_2	2.781 ± 0.165	2.748 ± 0.156	2.702 ± 0.142	2.571 ± 0.159	2.509 ± 0.156	2.359 ± 0.149
A_3	1.975 ± 0.172	2.109 ± 0.159	2.135 ± 0.144	1.978 ± 0.162	1.920 ± 0.161	1.747 ± 0.151
A_4	1.403 ± 0.136	1.278 ± 0.125	1.248 ± 0.112	1.098 ± 0.131	1.088 ± 0.131	0.886 ± 0.124
A_5	0.675 ± 0.116	0.757 ± 0.107	0.667 ± 0.092	0.670 ± 0.107	0.565 ± 0.107	0.593 ± 0.094
$P(\chi^2)$	0.62	0.63	0.56	0.89	0.62	0.52
	1134 MeV/c	1153 MeV/c	1174 MeV/c	1183 MeV/c	1226 MeV/c	
σ_{K^-p} (mb)	17.47 ± 0.70	17.63 ± 0.67	17.00 ± 0.71	16.15 ± 0.68	12.40 ± 0.79	
A_0	1.173 ± 0.047	1.212 ± 0.046	1.200 ± 0.050	1.152 ± 0.048	0.930 ± 0.059	
A_1	1.857 ± 0.122	2.007 ± 0.119	2.041 ± 0.129	1.872 ± 0.123	1.624 ± 0.152	
A_2	2.436 ± 0.163	2.555 ± 0.160	2.478 ± 0.171	2.274 ± 0.167	2.064 ± 0.199	
A_3	1.737 ± 0.168	1.928 ± 0.164	1.762 ± 0.181	1.683 ± 0.172	1.365 ± 0.216	
A_4	0.925 ± 0.137	1.121 ± 0.134	1.141 ± 0.149	0.936 ± 0.146	0.891 ± 0.181	
A_5	0.569 ± 0.107	0.652 ± 0.101	0.470 ± 0.116	0.644 ± 0.111	0.231 ± 0.151	
$P(\chi^2)$	0.70	0.46	0.40	0.90	0.09	

Table 2b
Same as table 2a for $n = 6$.
$d\sigma/d\Omega = \lambda\!\!\!^{-2} \Sigma_n A_n P_n(\cos\theta)$ for $n = 6$.

	777 MeV/c	806 MeV/c	838 MeV/c	853 MeV/c	874 MeV/c	894 MeV/c
σ_{K^-p} (mb)	18.70 ± 0.79	20.45 ± 0.95	19.53 ± 0.94	19.39 ± 0.79	20.31 ± 0.77	21.66 ± 0.85
A_0	0.712 ± 0.030	0.825 ± 0.038	0.837 ± 0.040	0.854 ± 0.035	0.928 ± 0.035	1.024 ± 0.040
A_1	1.125 ± 0.079	1.254 ± 0.100	1.154 ± 0.104	1.231 ± 0.091	1.269 ± 0.093	1.355 ± 0.105
A_2	1.142 ± 0.110	1.381 ± 0.140	1.437 ± 0.146	1.401 ± 0.128	1.541 ± 0.131	1.720 ± 0.148
A_3	0.493 ± 0.123	0.677 ± 0.158	0.730 ± 0.164	0.758 ± 0.143	0.727 ± 0.144	0.791 ± 0.163
A_4	0.261 ± 0.120	0.383 ± 0.156	0.445 ± 0.164	0.422 ± 0.138	0.492 ± 0.140	0.434 ± 0.160
A_5	0.236 ± 0.093	0.344 ± 0.121	0.315 ± 0.130	0.350 ± 0.108	0.321 ± 0.106	0.304 ± 0.121
A_6	0.097 ± 0.067	0.163 ± 0.092	0.117 ± 0.105	0.099 ± 0.081	0.091 ± 0.082	0.019 ± 0.096
$P(\chi^2)$	0.40	0.86	0.89	0.65	0.79	0.57
	904 MeV/c	916 MeV/c	935 MeV/c	954 MeV/c	970 MeV/c	991 MeV/c
σ_{K^-p} (mb)	20.71 ± 0.82	20.85 ± 0.82	20.12 ± 0.76	20.64 ± 0.86	20.72 ± 0.82	22.15 ± 0.83
A_0	0.996 ± 0.039	1.023 ± 0.040	1.018 ± 0.038	1.077 ± 0.045	1.107 ± 0.044	1.222 ± 0.046
A_1	1.322 ± 0.104	1.327 ± 0.106	1.240 ± 0.101	1.340 ± 0.118	1.349 ± 0.117	1.554 ± 0.122
A_2	1.828 ± 0.148	1.953 ± 0.150	1.946 ± 0.144	2.158 ± 0.166	2.300 ± 0.165	2.706 ± 0.172
A_3	0.836 ± 0.159	0.960 ± 0.164	0.965 ± 0.155	1.178 ± 0.181	1.216 ± 0.176	1.755 ± 0.181
A_4	0.498 ± 0.153	0.700 ± 0.160	0.730 ± 0.151	0.836 ± 0.176	0.917 ± 0.171	1.447 ± 0.171
A_5	0.237 ± 0.108	0.333 ± 0.118	0.446 ± 0.108	0.448 ± 0.129	0.372 ± 0.122	0.771 ± 0.117
A_6	0.012 ± 0.083	0.152 ± 0.096	0.086 ± 0.088	0.035 ± 0.107	0.002 ± 0.101	0.232 ± 0.094
$P(\chi^2)$	0.70	0.79	0.38	0.57	0.19	0.91

Table 2b (continued)

$d\sigma/d\Omega = \lambda^2 \Sigma_n A_n P_n(\cos\theta)$ for $n = 6$.

	1022 MeV/c	1044 MeV/c	1061 MeV/c	1080 MeV/c	1102 MeV/c	1117 MeV/c
σ_{K^-p} (mb)	22.15 ± 0.98	21.46 ± 0.89	20.56 ± 0.80	18.74 ± 0.83	18.77 ± 0.80	17.82 ± 0.75
A_0	1.279 ± 0.057	1.279 ± 0.054	1.254 ± 0.049	1.173 ± 0.053	1.210 ± 0.051	1.171 ± 0.049
A_1	1.637 ± 0.151	1.623 ± 0.144	1.711 ± 0.133	1.644 ± 0.141	1.686 ± 0.137	1.772 ± 0.131
A_2	2.753 ± 0.211	2.877 ± 0.200	2.781 ± 0.185	2.506 ± 0.195	2.457 ± 0.190	2.358 ± 0.182
A_3	1.943 ± 0.226	2.252 ± 0.214	2.225 ± 0.196	1.901 ± 0.213	1.860 ± 0.207	1.744 ± 0.200
A_4	1.356 ± 0.226	1.443 ± 0.214	1.343 ± 0.196	1.015 ± 0.213	1.020 ± 0.193	0.885 ± 0.184
A_5	0.640 ± 0.226	0.853 ± 0.214	0.730 ± 0.196	0.612 ± 0.213	0.515 ± 0.148	0.589 ± 0.140
A_6	− 0.052 ± 0.226	0.128 ± 0.214	0.068 ± 0.196	− 0.065 ± 0.213	− 0.056 ± 0.117	− 0.000 ± 0.104
$P(\chi^2)$	0.58	0.65	0.51	0.87	0.57	0.46

	1134 MeV/c	1153 MeV/c	1174 MeV/c	1183 MeV/c	1226 MeV/c
σ_{K^-p} (mb)	17.55 ± 0.79	17.23 ± 0.76	16.46 ± 0.79	15.89 ± 0.75	11.81 ± 0.83
A_0	1.179 ± 0.053	1.185 ± 0.053	1.161 ± 0.055	1.133 ± 0.054	0.886 ± 0.061
A_1	1.874 ± 0.142	1.928 ± 0.141	1.931 ± 0.146	1.818 ± 0.142	1.500 ± 0.161
A_2	2.461 ± 0.196	2.437 ± 0.195	2.296 ± 0.203	2.198 ± 0.196	1.820 ± 0.221
A_3	1.768 ± 0.216	1.786 ± 0.214	1.551 ± 0.222	1.582 ± 0.218	1.075 ± 0.248
A_4	0.960 ± 0.202	0.972 ± 0.214	0.898 ± 0.222	0.832 ± 0.218	0.465 ± 0.251
A_5	0.595 ± 0.156	0.538 ± 0.214	0.269 ± 0.222	0.558 ± 0.218	− 0.079 ± 0.251
A_6	0.027 ± 0.118	− 0.112 ± 0.214	− 0.205 ± 0.222	− 0.086 ± 0.218	− 0.354 ± 0.251
$P(\chi^2)$	0.64	0.44	0.22	0.93	0.65

b) resonant amplitudes: the non-relativistic Breit-Wigner amplitude was used,

$$T_R = \frac{x_e}{\epsilon - i}, \quad \text{where} \quad x_e = \frac{\Gamma_e}{\Gamma} \quad \text{and} \quad \epsilon = \frac{E_R - E}{\frac{1}{2}\Gamma}, \tag{2}$$

with an energy dependent width [10]

$$\Gamma(E) = \Gamma_R \frac{(kr)^{2l+1} \; D_l(k_R r)}{(k_R r)^{2l+1} \; D_l(kr)}. \tag{3}$$

In these expressions E is the total c.m. energy, E_R the mass of the resonance, Γ_R the width of the resonance at c.m. momentum k_R, r the radius of interaction taken as 1 fm, and $(kr)^{2l}/D_l(kr)$ the centrifugal barrier factor.

c) Superposition of non-resonant and resonant amplitudes: We describe the partial wave amplitude for this case by

$$T = T_B + T_R \, e^{2i\delta}, \tag{4}$$

where δ is an unspecified real phase, left as a free parameter. This amplitude differs from that of ref. [8], where the phase angle was taken to correspond to the complex phase of T_B.

The data used in the fit were:

1) The $K^-p \to K^-p$ and $K^-p \to \bar{K}^0n$ [7] differential cross sections, $d\sigma/d\Omega$, at twenty-three momenta between 777 and 1226 MeV/c.

2) The $K^-p \to K^-p$ polarization, $P(\theta)$, at 982, 1082, 1142, and 1212 MeV/c, respectively [2].

3) The total K^-p cross sections, σ_{tot}, at 26 momenta between 720 and 1226 MeV/c [11], interpolated to correspond to our K^- momenta.

As previously noted in ref. [1], it is felt that the use of the coefficients of the Legendre polynomial expansion of the differential cross sections as input data for a partial wave analysis of the $K^-p \to K^-p$ data, in particular, leads to difficulties associated with the truncation of the Legendre series at a particular order. We have chosen here to bypass the Legendre expansion, as done in ref. [1] (method B), and to perform a partial wave fit directly to the σ_{tot}, $d\sigma/d\Omega$ and $P(\theta)$ data themselves. With the above selection, there are 1483 data points available for the fit.

The search for the set of partial wave amplitudes which would give the best interpretation of the data was carried out using the following procedures:

a) A basic set of amplitudes was taken as starting point. The partial waves S_{01} through D_{03} contained at least a non-resonant amplitude. A minimal set of resonant contributions was also included. Within the momentum region covered by this experiment resonant amplitudes with free parameters were introduced to correspond to the well known resonances $D_{03}(1690)$, $D_{15}(1765)$, $F_{05}(1815)$. For two resonances falling respectively at the lower and upper ends of our region, $S_{01}(1670)$ and $F_{15}(1910)$, the mass and width were kept fixed while the elasticity (and phase angle for $S_{01}(1670)$) was left free to vary. Finally, the parameters of the resonant

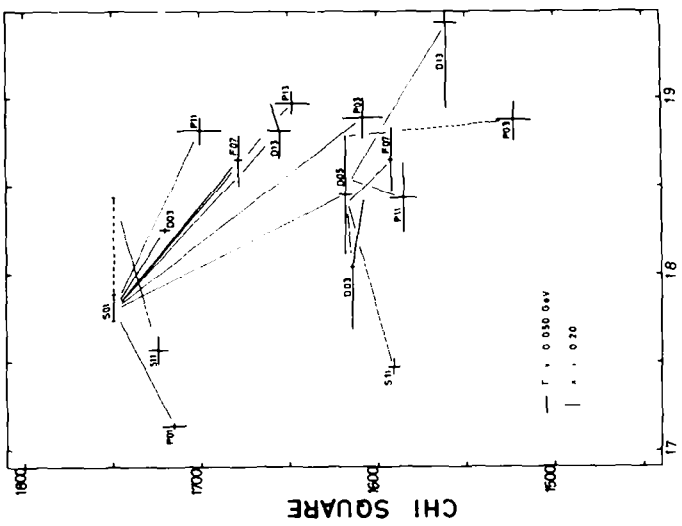

Fig. 2b. Continuation of the S_{01} branch of fig. 2a with the addition of a second and third resonance.

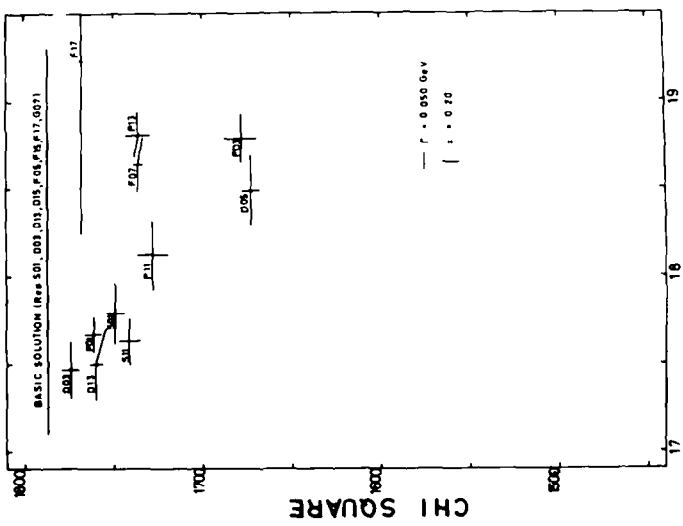

Fig. 2a. Diagrams indicating the improvement in χ^2 following the addition of one resonance to the set of resonant partial waves indicated as "basic solution". Plotted are the χ^2 of each solution versus the fitted mass of the resonance. Horizontal and vertical bars correspond to the resonance width and elasticity, respectively.

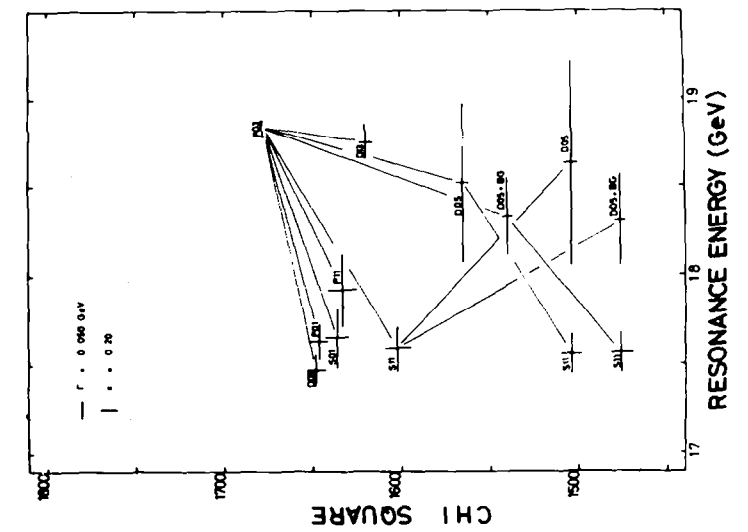

Fig. 2d. Continuation of the P_{03} branch of fig. 2a with the addition of a second and third resonance.

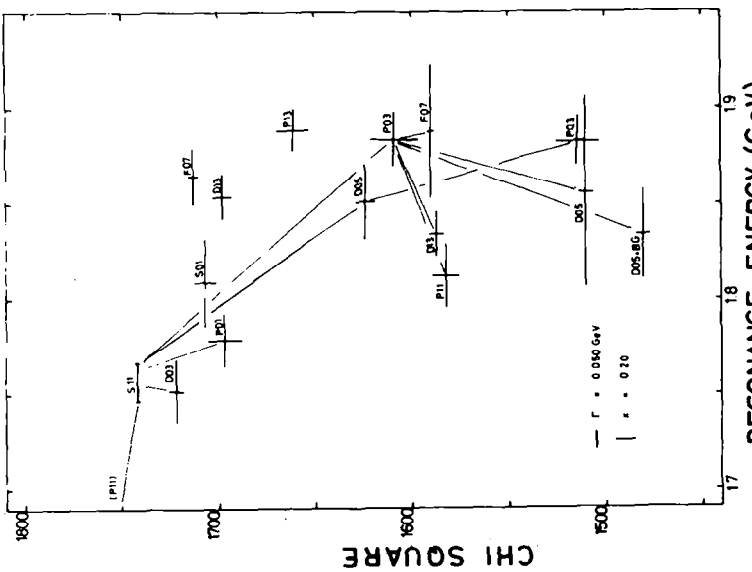

Fig. 2c. Continuation of the S_{11} branch of fig. 2a with the addition of a second and third resonance.

states $D_{13}(1660)$, $F_{17}(2025)$, and $G_{07}(2100)$, more remote from the energy range of this analysis, were taken as fixed.

This basic model contains 41 free parameters, yielding a χ^2 of 1787 after minimization, when the expected χ^2 is 1442, or a discrepancy of ~ 6.5 standard deviations.

b) One additional resonant contribution was then added to the basic set in a), to each of the partial waves S_{01} through F_{17} in turn. The results of these minimizations are shown in fig. 2a, where the χ^2 of the fit plotted versus the fitted mass, width and elasticity. As can be seen, the best fits are obtained when a resonance is added either to the P_{03} or D_{05} states.

c) Starting from any one of the solutions obtained in b), a second resonance was added to the model, testing its assignment to each of the partial waves S_{01} through F_{17}. The search has been similarly extended to include a third additional resonance. Figs. 2b-2d display, as examples, graphical descriptions of these searches for the families generated by the addition to the basic set a) of S_{01}, S_{11}, or P_{03} resonance respectively. Each final configuration of the basic solution with 3 added resonances can be reached via six different paths.

The best solution is achieved when adding to the basic set of amplitudes in a), three additional resonances in the states S_{11}, P_{03}, and D_{05}, together with a small non-resonant term in the latter. The lowest χ^2 thus obtained is 1480 against 1424 expected, representing an improvement of 5.5σ over set a). The reduction in χ^2 resulting from the inclusion of any of these resonances is significant. While the addition of an S_{11} state reduces the χ^2 typically by $\sim 1\sigma$, that of a P_{03} or D_{05} lowers the χ^2 by $\sim 2\sigma$. As it can be appreciated from figs. 2c and 2d, the final location on the energy scale at which each of the above states is demanded by the fits, is to a large extent independent of the order in which these resonances are added to the model.

The fitted parameters of the best solution are given in table 3. The partial wave amplitudes S_{01} through P_{13} are displayed in fig. 3, while the fits to the angular distributions of $K^-p \to K^-p$ and $K^-p \to \bar{K}^0n$ are shown as dashed curves in figs. 1a and 1b respectively. The polarization data of ref. [2] are shown together with our fit in fig. 4, and the fit to the total K^-p cross sections is given in fig. 5.

2.3. *Discussion*

Concerning the three additional states required by the above search, we note:

(i) D_{05}. A resonant state $\Lambda(1830)$ in this partial wave was first proposed by Armenteros et al. [3, 4], in an analysis of the $\bar{K}N$ channel and subsequently introduced also in the $\Sigma\pi$ channel [5]. In the former channel, however, the evidence for this state so far has been rather marginal. As mentioned above, the inclusion of this resonance in our fit improves the χ^2 by about two standard deviations. As can be seen in figs. 2c and 2d, a further improvement in χ^2 by half a standard deviation is achieved by adding a non-resonant term (which turned out to be small) to the resonant amplitude. A more significant gain is perhaps represented by the fact that in so doing,

Table 3

Parameters of the best solution discussed in the text. The non-resonant partial waves were parameterized as $a + b(p_K - 1)$ where p_K is the K^- lab momentum in GeV/c. The resonant partial waves had a Breit-Wigner form; in addition, when background was included in the same partial wave, the resonant amplitude was multiplied by a phase $e^{2i\delta}$. The parameters within brackets were kept fixed throughout the fit.

Non-resonant amplitudes	Re a	Im a	Re b	Im b
S_{01}	-0.24 ± 0.05	0.71 ± 0.02	0.14 ± 0.18	-0.63 ± 0.16
S_{11}	0.10 ± 0.02	0.66 ± 0.03	-0.59 ± 0.10	0.95 ± 0.15
P_{01}	-0.04 ± 0.02	0.47 ± 0.02	-0.71 ± 0.30	-0.08 ± 0.20
P_{11}	0.08 ± 0.03	0.26 ± 0.03	-0.95 ± 0.16	0.29 ± 0.23
P_{03}	0.28 ± 0.02	0.20 ± 0.02	-0.04 ± 0.10	0.41 ± 0.15
P_{13}	0.07 ± 0.03	0.16 ± 0.02	-0.47 ± 0.15	0.38 ± 0.10
D_{03}	0.00 ± 0.02	-0.02 ± 0.02	0.10 ± 0.10	0.38 ± 0.12
D_{05}	0.05 ± 0.03	0.02 ± 0.02	0.04 ± 0.06	0.08 ± 0.05

Resonant amplitudes	Mass (MeV)	Width (MeV)	Elasticity (x)	Phase angle 2δ (rad)
S_{01}	(1676)	(26)	0.39 ± 0.05 *	3.29 ± 0.25
S_{11}	1757 ± 10	55 ± 20	0.12 ± 0.05	0.00 ± 0.10
P_{03}	1883 ± 15	80 ± 20	0.25 ± 0.05	1.06 ± 0.20
D_{03}	1688 ± 3	64 ± 5	0.33 ± 0.04	0.10 ± 0.06
D_{13}	(1665)	(30)	(0.025)	-
D_{05}	1831 ± 10	104 ± 25	0.05 ± 0.02	0.00 ± 0.10
D_{15}	1770 ± 6	132 ± 20	0.36 ± 0.05	-
F_{05}	1818 ± 2	90 ± 8	0.63 ± 0.02	-
F_{15}	(1906)	(60)	0.11 ± 0.03	-
F_{17}	(2026)	(130)	(0.135)	-
G_{07}	(2100)	(145)	(0.305)	-

* See comment at the end of sect. 2.

the mass and width of the D_{05} resonance became compatible with the parameters found in the analysis of the $\Sigma\pi$ final state [5, 12]. Our best parameters for this state are M = 1831 ± 10 MeV, Γ = 104 ± 25 MeV, and x = 0.05 ± 0.02. Its accepted SU(3) classification is a member of the $\frac{5}{2}^-$ octet, with N(1680), Σ(1760) and Ξ(1930).

(ii) P_{03}. Our search favors the presence of a resonant amplitude in this partial wave, with parameters M = 1883 ± 15 MeV, Γ = 80 ± 20 MeV, x = 0.25 ± 0.05, phase angle 2δ = 1.06 ± 0.20 rad. The possible existence

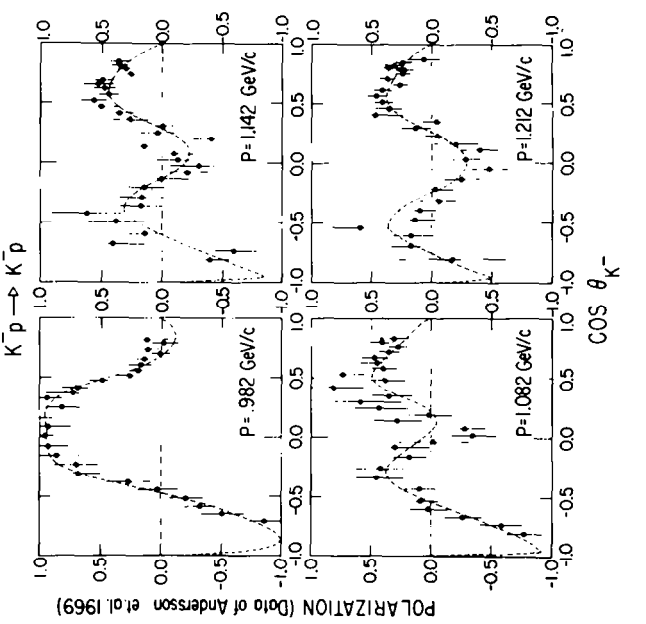

Fig. 4. The polarization differential cross sections of ref. [2] with the best partial wave fit discussed in the text.

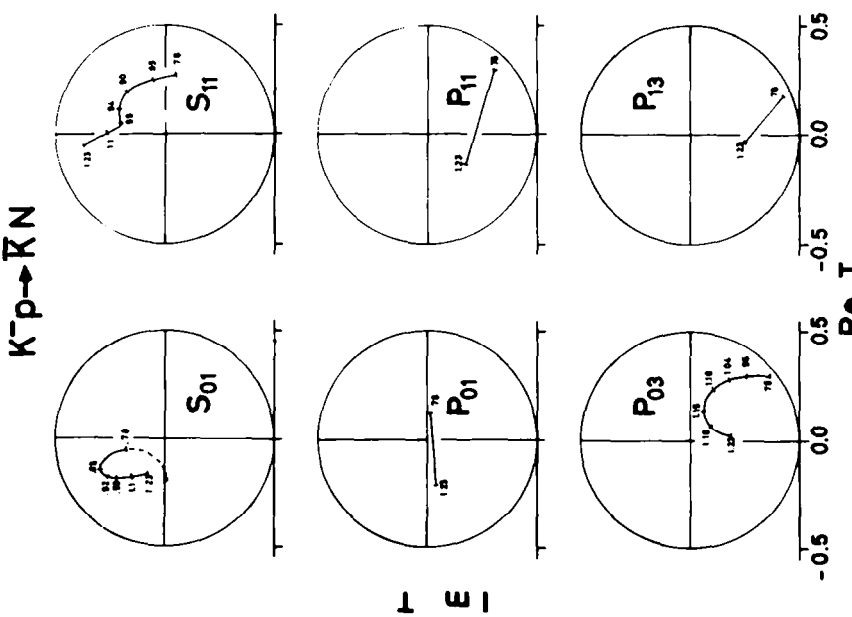

Fig. 3. Argand diagram for the S and P partial wave amplitudes of the best solution.

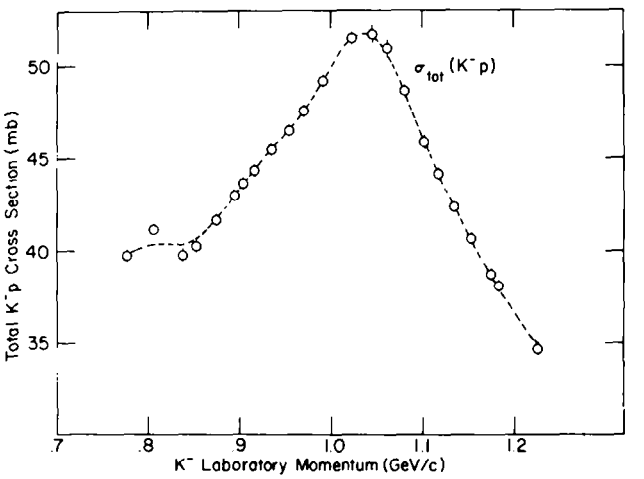

Fig. 5. Plot of σ_{tot} used in the fit. The dashed curve is calculated with the parameters of the best partial wave solution.

of an F_{07} state at approximately this energy was proposed in previous analyses of the $\bar{K}N$ channel [4]. The present fit indicates a clear preference for a $\frac{3}{2}^+$ assignment, rather than $\frac{7}{2}^+$, for $\Lambda(1870)$. With the old $\frac{7}{2}^+$ assignment, $\Lambda(1870)$ would have been the only state to fall significantly above the leading trajectory in a Chew-Frautschi plot. The new J^P assignment removes this peculiarity. A $\frac{3}{2}^+$ octet of baryons in this mass region could belong to the $(56, 2^+)$ SU(6) × 0(3) supermultiplet [13].

(iii) S_{11}. A mass value consistently close to 1760 MeV was obtained for a resonant state in this partial wave. Its best parameters are $M = 1757 \pm 10$ MeV, $\Gamma = 55 \pm 20$ MeV, $x = 0.12 \pm 0.05$. In the $\Lambda\pi^0$ channel, resonant behavior of the S_{11} partial wave has been reported [14] at approximately 1730 MeV, as a result of an energy independent partial wave analysis. The width found in this channel is ~80 MeV and the amplitude at resonance is ~0.25. In previous analyses of SU(3) baryon phenomenology [15, 16] it has been tentatively assumed that both the above effects could be associated with the $\Sigma\eta$ threshold enhancement [17, 18] and, therefore, as decay modes of the Σ member of the $\frac{1}{2}^-$ Nη octet. Alternatively, Greenberg [13] has suggested that $\frac{1}{2}^-$ $\Sigma(1760)$ might be a member of a decuplet in the $(70, 1^-)$, SU(6) × 0(3) supermultiplet. Several inconsistencies beset either assignment. Following the analysis of the $\frac{1}{2}^-$ octet in refs. [15, 16], the octet assignment for $\Lambda\pi(1730)$ is preferred by the observed sign (-) of the $\Lambda\pi$ resonant amplitude. The total width of the state, predicted from the decay rates of N(1525) and $\Lambda(1670)$ including singlet-octet mixing of the latter with $\Lambda(1405)$, should be much larger (~400 MeV) than the observed 50 - 80 MeV. The $\bar{K}N$ decay rate, in particular, should be a factor of 20 larger than observed here, and a predicted large $\Sigma\pi$ resonant amplitude is not evident in the results of ref. [14]. If a decuplet assignment is invoked, this cannot be extended to include the $\Lambda\pi$ decay

mode because of the wrong sign of the resonant amplitude in this channel. The $\bar{K}N$ and $\Sigma\eta$ decay rates, as well as the total width, could be, however, reconciled under this hypothesis.

The present situation could be construed, in fact, as providing some evidence for the existence of at least two $\frac{1}{2}^-$ states, one belonging to an octet, the other to a decuplet, with masses rather close to each other. Several questions would still be unanswered in this case, in particular, as to the fate of the $\bar{K}N$ and $\Sigma\pi$ decay modes of the octet member. Some of these difficulties could be accommodated by recourse to octet-decuplet mixing of the $\frac{1}{2}^-$ Σ states. Clarification of this rather complicated situation clearly awaits for more detailed and accurate experimental data.

(iv) Other Resonant States. An early attempt at analyzing our data along the present lines had given an indication, together with $S_{11}(1760)$, for a possible $S_{01}(1750)$ [19]. Its inclusion in the present fit as a fourth resonance in addition to the basic set of amplitudes described above would further reduce the χ^2 by $\sim 0.5 - 1\sigma$. Although the existence of such a resonance still remains compatible with our analysis of the data, we feel that the evidence for the states discussed above is more compelling in terms of relative priority. This problem was recently revived by the results of Bricman et al. [20] where a possible S_{01} state at ~ 1850 MeV seems likely.

The resonant parameters of the "well known states", are generally in agreement with those of previous analyses. The elasticity of $S_{01}(1670)$ as obtained here ($x = 0.39 \pm 0.05$) is at variance with the generally accepted values in the range 0.14 - 0.23 [8, 9, 15]. If in our best fit a value of $x = 0.18$ is imposed, the χ^2 increases by 70 points, but all partial waves other than the S_{01} are practically unaffected. Since $S_{01}(1670)$ falls outside the energy range covered by this analysis, the separation between resonant and background amplitude is not well constrained in that region. Therefore our value for the elasticity of $S_{01}(1670)$ while not invalidating our fit should not be considered for the purpose of averaging resonant parameters.

3. EXPERIMENTAL TEST OF $\bar{K}N$ DISPERSION RELATIONS

3.1. *Empirical determination of* $|\mathrm{Re}f(0)|/\mathrm{Im}f(0)$

Our $K^-p \to K^-p$ data in the momentum interval 777 - 1226 MeV/c, together with those of ref. [21] between 436 and 793 MeV/c, enable a detailed comparison to be made of the empirical ratio $|\alpha| = |\mathrm{Re}f(0)|/\mathrm{Im}f(0)$ with the predictions of several dispersion relation calculations for this quantity. Such a comparison can be made in two ways:

a) On the basis of the values of $|\alpha|$ determined from

$$\left.\frac{d\sigma}{d\Omega}\right]_{\theta=0} = |f(0)|^2 = (\mathrm{Re}f(0))^2 + (\mathrm{Im}f(0))^2 , \tag{5}$$

$$(\mathrm{Im}f(0))^2 = \sigma_{tot}^2/(4\pi\lambda\!\!\!^{-})^2 . \tag{6}$$

This approach is beset with considerable uncertainty due to the limitations in extrapolating the truncated angular distribution to the forward direction.

Table 4a

The forward and backward points as extrapolated from Legendre fits to the differential $K^-p \to K^-p$ cross sections for the minimum order $n = n_{min}$ of the expansion giving an acceptable fit. Data from this experiment. Values of $(\mathrm{Im}\, f(0))^2$ from σ_{tot} [11] through the optical theorem and of $|\mathrm{Re}\, f(0)|/\mathrm{Im}\, f(0)$ are also presented.

P (GeV/c)	$\frac{d\sigma}{d\Omega}\Big\vert_{\theta=0}$ (mb/sr)	$\lvert \mathrm{Im}\, f(0)\rvert^2$ (mb/sr)	$\left\lvert\frac{\mathrm{Re}\, f(0)}{\mathrm{Im}\, f(0)}\right\rvert$	$\frac{d\sigma}{d\Omega}\Big\vert_{\theta=2\pi}$ (mb/sr)	n
0.777	5.95 ± 0.54	4.79	$0.49^{+0.11}_{-0.13}$	0.82 ± 0.13	4
0.806	6.46 ± 0.65	5.45	$0.43^{+0.12}_{-0.17}$	0.97 ± 0.18	4
0.838	6.73 ± 0.65	5.39	$0.50^{+0.11}_{-0.14}$	1.37 ± 0.20	4
0.853	8.17 ± 0.82	5.69	$0.66^{+0.10}_{-0.12}$	0.68 ± 0.16	5
0.874	8.42 ± 0.80	6.38	$0.57^{+0.10}_{-0.13}$	1.15 ± 0.17	5
0.894	9.32 ± 0.88	6.97	$0.58^{+0.10}_{-0.12}$	1.24 ± 0.20	5
0.904	9.41 ± 0.81	7.31	$0.54^{+0.09}_{-0.12}$	1.52 ± 0.18	5
0.916	9.05 ± 0.84	7.69	$0.42^{+0.12}_{-0.16}$	1.69 ± 0.22	5
0.935	9.32 ± 0.76	8.39	$0.33^{+0.12}_{-0.22}$	1.63 ± 0.19	5
0.954	10.49 ± 0.87	9.05	$0.40^{+0.10}_{-0.15}$	1.69 ± 0.23	5
0.970	10.81 ± 0.83	9.69	$0.34^{+0.11}_{-0.16}$	2.07 ± 0.22	5
0.991	11.68 ± 0.78	10.60	$0.32^{+0.10}_{-0.15}$	1.83 ± 0.19	5
1.022	13.48 ± 0.96	12.11	$0.34^{+0.10}_{-0.16}$	1.61 ± 0.24	5
1.044	12.94 ± 0.87	12.79	$0.11^{+0.17}_{-0.11}$	1.16 ± 0.21	5
1.061	12.59 ± 0.77	12.62	< 0.24	0.95 ± 0.16	5
1.080	11.69 ± 0.84	11.82	< 0.25	0.66 ± 0.17	5
1.102	11.16 ± 0.81	10.77	$0.19^{+0.15}_{-0.19}$	0.76 ± 0.17	5
1.117	10.34 ± 0.75	10.23	$0.10^{+0.19}_{-0.10}$	0.37 ± 0.12	5

Table 4a (continued)

P (GeV/c)	$\frac{d\sigma}{d\Omega}\Big\|_{\theta=0}$ (mb/sr)	$\|\mathrm{Im}\, f(0)\|^2$ (mb/sr)	$\left\|\frac{\mathrm{Re}\, f(0)}{\mathrm{Im}\, f(0)}\right\|$	$\frac{d\sigma}{d\Omega}\Big\|_{\theta=2\pi}$ (mb/sr)	n
1.134	10.32 ± 0.81	9.60	$0.27^{+0.13}_{-0.27}$	0.44 ± 0.15	5
1.153	10.12 ± 1.13	9.07	$0.34^{+0.15}_{-0.34}$	0.27 ± 0.14	6
1.174	8.92 ± 1.18	8.42	$0.24^{+0.20}_{-0.24}$	0.45 ± 0.18	6
1.183	8.98 ± 1.13	8.23	$0.30^{+0.18}_{-0.30}$	0.14 ± 0.14	6
1.226	5.64 ± 1.25	7.20	-	0.34 ± 0.25	6

b) On the basis of the values of α deduced from the best energy dependent partial wave fit. This approach is more reliable in view of the continuity imposed on the momentum dependence of the partial waves, provided the fit is obtained, as done here, through a fit to the differential cross sections instead of a fit to the coefficients of the Legendre expansions of the differential cross sections.

The critical choice to be made in a) is that of the minimum order $n_{\min}$ in the Legendre expansion, required to obtain a reliable extrapolation to $d\sigma/d\Omega]_{\theta=0}$. As well known, in fact, the extrapolated values of $d\sigma/d\Omega]_{\theta=0}$ generally increase for $n > n_{\min}$, in spite of the fact that $d\sigma/d\Omega$ is measured here over most of the angular range ($-1 \leq \cos\theta_K \leq 0.95$). Our previous determinations of $d\sigma/d\Omega]_{\theta=0}$ as well as those of ref. [21] have been critically reappraised with this consideration in mind. Included in table 4a and 4b are the forward and backward differential cross sections corresponding to the minimum order of expansion giving an "acceptable" fit ($p(\chi^2) > 0.05$). These data are also shown in fig. 6.

The total cross sections adopted for the determination of $(\mathrm{Im}\, f(0))^2$ are those of ref. [11] for the region above 600 MeV/c. The cross sections in the region 436 - 600 MeV/c represent a weighted average of the results of refs. [21, 22].

The values of $|\alpha|$ derived from these data are contained in table 4a and 4b and shown in fig. 7. Fig. 7 also indicates the behavior of α according to the best partial-wave analysis described in this paper, and that corresponding to the analysis of ref. [8].

3.2. *Dispersion relation calculations*

The theoretical predictions which were chosen for comparison are representative of different approaches to the technical difficulties which are peculiar to the calculation of $\bar{K}N$ dispersion relations. As is well known, these difficulties arise from the presence of inelastic thresholds and resonances below the $\bar{K}N$ threshold. Ultimately, the different

Table 4b
Same as table 4a for the data of ref. [21]. Values of $(\mathrm{Im}\, f(0))^2$ from the σ_{tot} data of refs. [21, 22].

P (GeV/c)	$\frac{d\sigma}{d\Omega}\Big\|_{\theta=0}$ (mb/sr)	$\|\mathrm{Im}\, f(0)\|^2$ (mb/sr)	$\left\|\frac{\mathrm{Re}\, f(0)}{\mathrm{Im}\, f(0)}\right\|$	$\frac{d\sigma}{d\Omega}\Big\|_{\theta=2\pi}$ (mb/sr)	n
0.793	7.36 ± 0.44	5.27	$0.63^{+0.06}_{-0.07}$	1.09 ± 0.14	4
0.773	7.03 ± 0.43	4.62	$0.72^{+0.06}_{-0.07}$	1.08 ± 0.14	4
0.761	7.23 ± 0.47	4.18	$0.85^{+0.07}_{-0.07}$	0.84 ± 0.15	4
0.740	4.84 ± 0.30	3.59	$0.59^{+0.07}_{-0.08}$	0.48 ± 0.10	3
0.719	4.39 ± 0.10	3.30	$0.57^{+0.08}_{-0.08}$	0.28 ± 0.10	3
0.699	4.03 ± 0.27	3.15	$0.53^{+0.07}_{-0.09}$	0.41 ± 0.10	3
0.677	3.55 ± 0.26	3.00	$0.43^{+0.09}_{-0.12}$	0.23 ± 0.09	3
0.658	3.55 ± 0.26	2.93	$0.46^{+0.09}_{-0.11}$	0.32 ± 0.09	3
0.637	3.62 ± 0.24	2.87	$0.51^{+0.08}_{-0.09}$	0.17 ± 0.07	3
0.617	3.47 ± 0.17	2.83	$0.48^{+0.05}_{-0.07}$	0.51 ± 0.08	2
0.597	3.23 ± 0.17	2.81	$0.39^{+0.07}_{-0.09}$	0.37 ± 0.07	2
0.573	2.92 ± 0.18	2.85	$0.16^{+0.14}_{-0.16}$	0.47 ± 0.07	2
0.554	3.14 ± 0.18	2.88	$0.30^{+0.09}_{-0.13}$	0.79 ± 0.09	2
0.534	3.00 ± 0.20	2.90	$0.19^{+0.13}_{-0.19}$	0.73 ± 0.10	2
0.514	3.26 ± 0.22	2.98 *	$0.31^{+0.10}_{-0.17}$	0.81 ± 0.10	2
0.495	3.28 ± 0.21	2.98 *	$0.32^{+0.09}_{-0.15}$	1.03 ± 0.11	2
0.475	3.10 ± 0.20	3.13 *	< 0.23	1.12 ± 0.11	2
0.455	3.43 ± 0.22	3.43 *	$0.00^{+0.25}$	1.67 ± 0.14	2
0.436	3.95 ± 0.29	3.88 *	$0.13^{+0.17}_{-0.13}$	2.80 ± 0.20	2

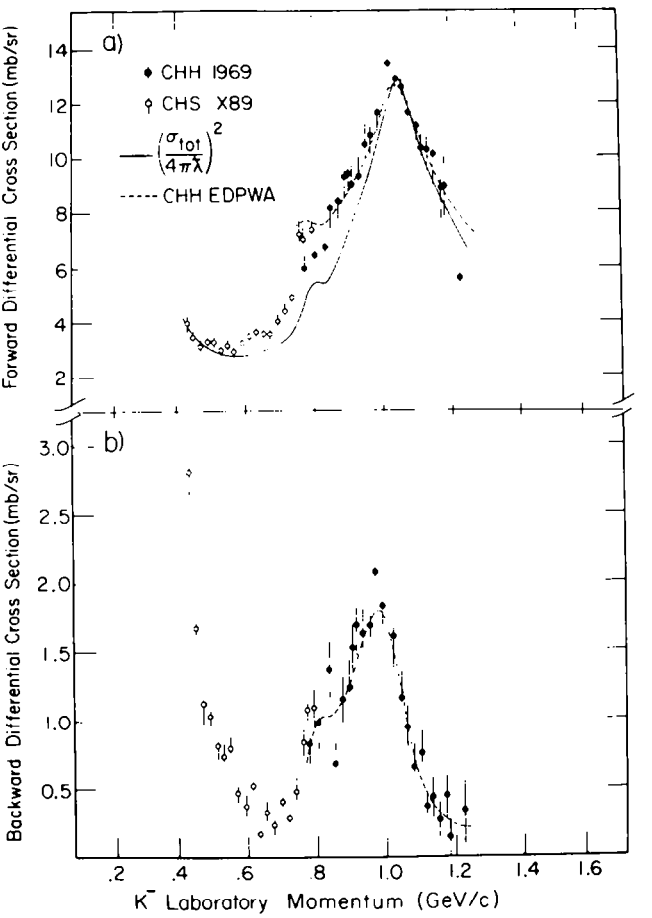

Fig. 6. Comparison of the forward and backward differential cross sections with $(\text{Im } f(0))^2$ and with the prediction from the best partial wave fit discussed here.

approaches to these complications rest upon how the low energy $\bar{K}N$ amplitude is parametrized. In fact, in order to derive the magnitude of the $\bar{K}\Lambda p$ and $\bar{K}\Sigma p$ coupling constants and in turn the ratio α, this amplitude must be continued below the $\bar{K}N$ threshold to the $\pi\Lambda$ threshold.

In Zovko's calculations [23] the low energy $\bar{K}N$ amplitude was given by

$$f(k, \theta) = \tfrac{1}{2} \frac{A_0}{1 - ikA_0} + \tfrac{1}{2} \frac{A_1}{1 - ikA_1} , \qquad (7)$$

where A_0 and A_1 are constant, complex scattering lengths. It is well known that A_0 is related to the location and width of the below-threshold resonance $\Lambda(1405)$ (S_{01}). Despite the apparent agreement with our partial wave solution, Zovko did not allow in his calculation for the P_{13} wave which would be the tail of the $\Sigma(1385)$. Lusignoli et al. [24] (LRVS), on the

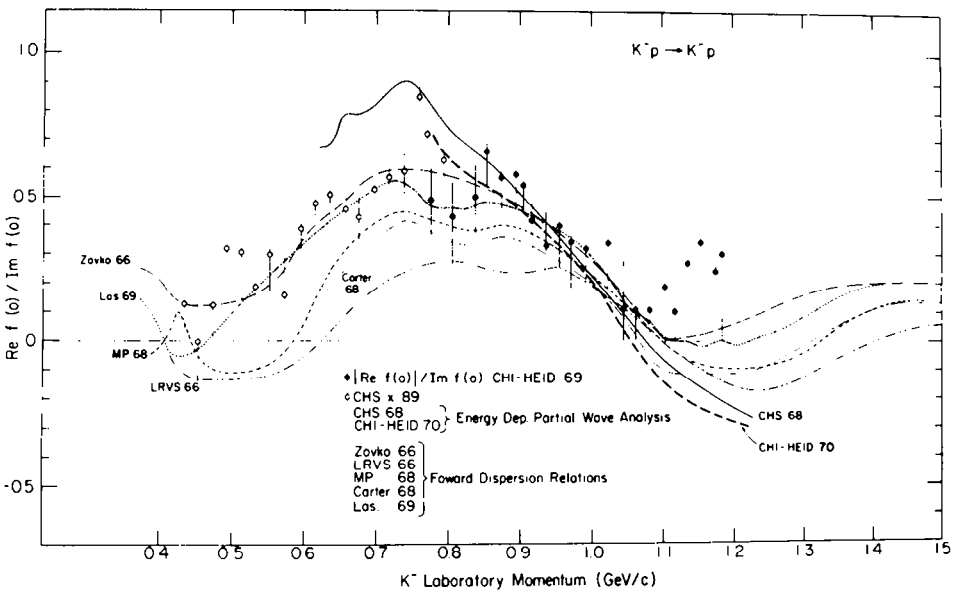

Fig. 7. The ratio $|\mathrm{Re}f(0)|/\mathrm{Im}\,f(0)$ from extrapolated forward differential cross sections and $\sigma_{tot}(K^-p)$ data. The predictions of our best solution and that of ref. [8] as various forward dispersion relation calculations are shown for comparison.

other hand, included in effective pole term for this resonance and computed a much lower value for α as seen in fig. 7.

Both the above calculations suffer from a shortcoming pointed out by Rood [25]. If the low energy amplitude is parametrized by the K-matrix formalism of Dalitz and Tuan [26], then A_0 and A_1 will actually have a momentum dependence. Carter [27] repeated essentially the LRVS calculation with Rood's criticism in mind. His results are very close to those of Martin and Poole [28] who suggested a modified dispersion relation which should not be quite so sensitive to the below-threshold region. All these authors used a $\bar{K}\Lambda N$ coupling constant $g^2_{\bar{K}\Lambda p} \approx 4 - 7$.

Recently one of us (T.L.) [29] has calculated α using the low energy amplitude and coupling constants of Kim [30]. These results are also shown in fig. 7. Kim fitted the available $\bar{K}N$ data from threshold to 550 MeV/c using an effective range K-matrix parametrization

$$K^{-1} = M + \tfrac{1}{2} qRq \ , \tag{8}$$

where M is a constant matrix, q is a diagonal matrix of channel ($\bar{K}N$, $\pi\Lambda$, $\pi\Sigma$) momenta, and R, a diagonal matrix of constant effective ranges. As Kim pointed out, the effective range parametrization in eq. (8) leads to a larger value for the S-wave amplitudes below threshold than eq. (7). This in turn is reflected in a larger value for $g^2_{\bar{K}\Lambda p} = 13 \pm 3$ [30]. (Kim's published result, ~16, should be corrected by m_p/m_Λ as pointed out by (among others) Chan and Meiere [31].)

Since in Kim's fit, data up to 550 MeV/c were included, P and D waves have to be considered. Several authors [32] have recently pointed out that this introduces a large number of undetermined parameters *. Furthermore, at the higher momenta the $\pi\pi\Lambda$ channel becomes significant, though Kim neglected it. Consequently, these authors have fitted the low energy $\bar{K}N$ data only up to 300 MeV/c with a constant K-matrix. They thus dropped the second term in eq. (8) and could reasonably neglect all partial waves higher than S. This gave a much lower value of $g^2_{\bar{K}\Lambda p} \approx 5 \pm 1$, and their curves for Re $f(0)$/Im $f(0)$ would most likely agree with those of Carter and of Martin and Poole.

We would like to emphasize one criticism of these constant K-matrix fits [32]. By this approach the fitted S-wave is continued into the unphysical region over a momentum range three times as wide as that over which it was determined above the elastic threshold. As Kim has indicated [30], although eqs. (7) and (8) give nearly identical results for the S-wave from threshold to 300 MeV/c, they differ considerably below the location of $\Lambda(1405)$. Despite the valid criticism of his parametrizations, Kim is the only author who has been consistent in this regard. Ultimately, the choice between constant K-matrix and effective K-matrix fits will require knowledge of partial waves at momenta from ~500 MeV/c to ~800 MeV/c. Clearly, the correct solution near threshold will have to extrapolate smoothly to the higher energy solutions [33].

There are other methods [34, 35] for determining $g^2_{\bar{K}\Lambda p}$ which in principle are relatively insensitive to the low energy data. In the work of Cutkosky and Deo [34] the residue of the $\Lambda+\Sigma$ poles is determined by a fit to one K^+p differential cross section with a set of "optimally convergent polynomials". Neglecting the mass differences of the hyperons, these authors obtained the result $g^2_{\bar{K}\Lambda p} + g^2_{\bar{K}\Sigma p} = 15^{+6}_{-4}$ and concluded that this result is consistent with Kim's value, $g^2_{\bar{K}\Lambda p} = 13 \pm 3$.

Recently, Martin and Perrin [35] have made a least-squares fit, based on a finite-energy dispersion relation, to the experimental real parts of the forward scattering amplitude obtaining $g^2_{\bar{K}\Lambda p} + 0.84\, g^2_{\bar{K}\Sigma p} = 8.8 \pm 3.0$ **. Although this is consistent with the result of ref. [30], they ruled out Kim's coupling constant because his K-matrix parametrization of the low-energy amplitude did not satisfy a consistency test provided by their analysis. In fact, the claim is made that only the constant scattering length parametrization satisfies such a test. This may indicate that the three-body final states, which are not readily treated in the K-matrix formalism, are considerably more important than is usually assumed. Most of the authors mentioned admit that systematic errors in these analyses are difficult to estimate. It is clear from the above discussion that a systematic effect

* In the K-matrix approach there will be parameters corresponding to $\pi\Sigma \rightarrow \pi\Sigma$, etc., reactions for which there are no data. As the number of partial waves increases, the number of these undetermined parameters also increases.

** The values of α tabulated by these authors essentially agree with those of ref. [28].

could lead to discrepancies in $g^2_{\bar{K}\Lambda p}$ by a factor of 2. These uncertainties are in turn reflected by the spread in the theoretical calculations shown in fig. 7.

3.3. *Comparison with experimental data*

With the above technical difficulties in mind, we now discuss fig. 7. Within the errors, the curves corresponding to the more recent dispersion relation calculations agree for the most part with the experimental values of $|\alpha|$. The spike in $|\alpha|$ at ~800 MeV/c reflects the effect of $D_{03}(1700)$ and, perhaps, the lack of a more detailed knowledge of the total cross section in that region. A considerable improvement in this comparison, over one previously reported [15], was brought about on one side by the use of more reliable total cross sections, in particular, below ~600 MeV/c, on the other by the more judicious choice of $n_{\min}$ of the Legendre expansion, used in the extrapolation procedure to obtain $d\sigma/d\Omega]_{\theta=0}$. On the latter point, we concur with the criticism of previous extrapolations as expressed by Martin and Perrin [35].

The curve for α corresponding to the present partial wave analysis also agrees reasonably well with several dispersion relation predictions. This is also the case for the earlier CHS solution [8] above ~800 MeV/c. The discrepancy between the latter and both the experimental values reported here and the theoretical predictions in the region 600 - 800 MeV/c stems, in our opinion, from the fact that the CHS fit was made to Legendre coefficients obtained from expansions of order greater than $n_{\min}$ in table 4b.

In conclusion, since both the dispersion relation calculations and the experimental determination of α involve rather delicate choices, the comparison of fig. 7 should be regarded as satisfactory. However, the sensitivity of the comparison is probably insufficient to indicate a preference amongst the various calculations.

REFERENCES

[1] B. Conforto, D. -M. Harmsen, T. Lasinski, R. Levi-Setti, M. Raymund, E. Burkhardt, H. Filthuth, E. Kluge, H. Oberlack and R. R. Ross, Nucl. Phys. B8 (1968) 265.

[2] S. Andersson, C. Daum, F. C. Erné, J. P. Lagnaux, J. C. Sens and F. Udo, CERN 14 Nov. 1969, Nucl. Phys. to be published.

[3] R. Armenteros, M. Ferro-Luzzi, D. W. G. Leith, R. Levi-Setti, A. Minten, R. D. Tripp, H. Filthuth, V. Hepp, E. Kluge, H. Schneider, R. Barloutaud, P. Granet, J. Meyer and J. P. Porte, paper presented at the 1966 Int. Conf. on high energy physics at Berkeley, see ref. [17].

[4] R. Armenteros, M. Ferro-Luzzi, D. W. G. Leith, R. Levi-Setti, A. Minten, R. D. Tripp, H. Filthuth, V. Hepp, E. Kluge, H. Schneider, R. Barloutaud, P. Granet, J. Meyer and J. -P. Porte, Nucl. Phys. B3 (1967) 592.

[5] R. Armenteros, M. Ferro-Luzzi, D. W. H. Leith, R. Levi-Setti, A. Minten, R. D. Tripp, H. Filthuth, V. Hepp E. Kluge, H. Schneider, R. Barloutaud, P. Granet, J. Meyer and J. -P. Porte, Phys. Letters 24B (1967) 198.

[6] B. Conforto, D. -M. Harmsen, T. Lasinski, R. Levi-Setti, M. Raymund, E. Burkhardt, H. Filthuth, S. Klein, H. Oberlack and H. Schleich, presented at the Lund Int. Conf. on elementary particles; paper 383 see R. Levi-Setti, rapporteur's talk on strange baryon resonances, conf. proc. (Berlingska Boktryckeriet, Lund, 1969).
[7] R. Armenteros, M. Ferro-Luzzi, D. W. G. S. Leith, R. Levi-Setti, A. Minten, R. D. Tripp, H. Filthuth, V. Hepp, E. Kluge, H. Schneider, R. Barloutaud, P. Granet, J. Meyer and J. -P. Porte, Nucl. Phys. B8 (1968) 233.
[8] R. Armenteros, P. Baillon, C. Bricman, M. Ferro-Luzzi, D. E. Plane, N. Schmitz E. Burkhardt, H. Filthuth, E. Kluge, H. Oberlack, R. R. Ross, R. Barloutaud, P. Granet, J. Meyer, J. -P. Porte, J. Prévost Nucl. Phys. B8 (1968) 195.
[9] R. Armenteros, P. Baillon, C. Bricman, M. Ferro-Luzzi, H. K. Nguyen, E. Pagiola, V. Pelosi, D. E. Plane, N. Schmitz, E. Burkhardt, H. Filthuth, E. Kluge, H. Oberlack, R. Barloutaud, P. Granet, J. Meyer, J. L. Narjoux, F. Pierre, J. -P. Porte and J. Prévost, presented at the Lund Int. Conf. on elementary particles (paper 225) see R. Levi-Setti, rapporteur talk on strange baryon resonances, conf. proc. (Berlingska Boktryckeriet, Lund, 1969) Also, CERN, Heidelberg collaboration, paper presented by D. E. Plane at the Duke Conf. on hyperon resonances, April 1970.
[10] R. D. Tripp, Baryon Resonances, In Proc. Int. school of physics, "Enrico Fermi" 1964 (Academic Press, New York).
[11] R. L. Cool, G. Giacomelli, T. F. Kycia, B. A. Leontic, K. K. Li, A. Lundby and J. Teiger, Phys. Rev. Letters 16 (1966) 1228;
D. V. Bugg R. S. Gilmore, K. M. Knight, D. C. Slater, G. H. Stafford, E. J. N. Wilson, J. D. Davies, J. D. Dowell, P. M. Hattersley, R. J. Homer, A. W. O'Dell, A. A. Carter, R. T. Tapper and K. F. Riley, Phys. Rev. 168 (1968) 1466.
[12] R. B. Bell, Phys. Rev. Letters 19 (1967) 936.
[13] O. W. Greenberg, rapporteur talk on resonance models, Proc. Lund Int. Conf. on elementary particles (Berlingska Boktryckeriet, Lund 1969).
[14] R. Armenteros, P. Baillon, C. Bricman, M. Ferro-Luzzi, H. K. Nguyen, E. Pagiola, V. Pelosi, D. E. Plane, N. Schmitz (CERN); E. Burkhardt, H. Filthuth, E. Kluge H. Oberlack (Heidelberg); R. Barloutaud, P. Granet, J. Meyer, J. L. Narjoux, F. Pierre, J. -P. Porte, J. Prévost (CEN Sacley), presented at the Lund Int. Conf. on elementary particles (paper 227); see R. Levi-Setti, rapporteur talk on strange baryon resonances, conf. proc. (Berlingska Boktrykeriet, Lund, 1969); Also, CERN-Heidelberg collaboration, paper presented by D. E. Plane at the Duke Conf. on hyperon resonances, April 1970.
[15] R. Levi-Setti, rapporteur talk on strange baryon resonances, Proc. Lund Int. Conf. on elementary particles (Berlingska Boktryckeriet, Lund, 1969).
[16] R. D. Tripp, Third Topical Conf. on particle physics, Honolulu, Hawaii, 1969, UCRL 19361 preprint.
[17] M. Ferro-Luzzi, rapporteur talk on baryon resonances with $S \neq 0$, Proc. 13th Int. Conf. on high energy physics, Berkeley, 1966 (University of California Press, 1967).
[18] J. Meyer, rapporteur talk on baryonic resonances with $S \neq 0$, Proc. of Heidelberg Int. Conf. on elementary particles, 1967 (North-Holland, Amsterdam, 1968).
[19] R. D. Tripp, rapporteur talk on strange baryon resonances, Proc. 14th Int. Conf. on high energy physics, Vienna 1968 (CERN, Geneva, 1968).
[20] C. Bricman, M. Ferro-Luzzi and J. P. Lagnaux, paper presented at the Duke Conf. on hyperon resonances, April 1970.
[21] R. Armenteros, P. Baillon, C. Bricman, M. Ferro-Luzzi, E. Pagiola, J. O. Petersen, D. E. Plane, N. Schmitz, E. Burkhardt, H. Filthuth E. Kluge, H. Oberlack, R. R. Ross, R. Barloutaud, P. Granet, J. Meyer, J. -P. Porte and J. Prévost, Nucl. Phys., to be published.

[22] D. V. Petersen, Thesis, University of Arizona, 1970, Presented by R. W. Jenkins at the Duke Conf. on hyperon resonances, April 1970.
[23] N. Zovko, Z. Phys. 196 (1966) 16; Phys. Letters 23 (1966) 143.
[24] M. Lusignoli, M. Restignoli, G. Violini and G. A. Snow, Nuovo Cimento 45A (1966) 792.
[25] H. P. C. Rood, CERN, preprint TH-733, December 1966.
[26] R. H. Dalitz and S. F. Tuan, Ann. of Phys. 10 (1960) 367.
[27] A. A. Carter, Cavendish Laboratory preprint 68/10.
[28] A. D. Martin and F. Poole, Phys. Letters 25B (1967) 343; Nucl. Phys. B4 (1968) 467.
[29] T. Lasinski, EFI Bubble Chamber Group report 1 (1969).
[30] J. K. Kim, Phys. Rev. Letters 19 (1967) 1074, 1079.
[31] C. H. Chan and F. T. Meiere, Phys. Rev. Letters 20 (1968) 568.
[32] B. R. Martin and M. Sakitt, Phys. Rev. 183 (1969) 1345;
A. D. Martin and G. G. Ross, University of Durham preprint, August 1969.
[33] For a further discussion of the point, see T. A. Lasinski, contribution to Duke Conf. on hyperon resonances, Duke University, April 1970.
[34] R. E. Cutkosky and B. B. Deo, Phys. Rev. Letters 20 (1968) 1271.
[35] A. D. Martin and R. Perrin, University of Durham preprint, February 1970.